Quaternary Science Reviews 167 (2017) 47–62

Contents lists available at ScienceDirect

Quaternary Science Reviews

journal homepage: www.elsevier.com/locate/quascirev

Evidence for orbital and North Atlantic climate forcing in alpine Southern California between 125 and 10 ka from multi-proxy analyses of Baldwin Lake

Katherine C. Glover [a, *], Glen M. MacDonald [a, b, g], Matthew E. Kirby [c], Edward J. Rhodes [d, e], Lora Stevens [f], Emily Silveira [c], Alexis Whitaker [g], Scott Lydon [a]

[a] Dept of Geography, University of California – Los Angeles, Los Angeles, CA, 90095, USA
[b] Dept of Ecology and Evolutionary Biology, University of California – Los Angeles, Los Angeles, CA, 90095, USA
[c] Department of Geological Sciences, California State University – Fullerton, Fullerton, CA, 92834, USA
[d] Department of Earth, Planetary, and Space Sciences, UCLA, Los Angeles, CA, 90095, USA
[e] Department of Geography, University of Sheffield, Sheffield, S10 2TN, UK
[f] Department of Geological Sciences, California State University – Long Beach, Long Beach, CA, 90840, USA
[g] Institute of Environment and Sustainability, 300 La Kretz, University of California – Los Angeles, Los Angeles, CA, 90095, USA

ARTICLE INFO

Article history:
Received 31 August 2016
Received in revised form
19 April 2017
Accepted 27 April 2017

Keywords:
Southern California
Summer insolation
Marine isotope stages
Dansgaard-Oeschger events
Hydroclimate
Paleoproductivity
San Bernardino Mountains
Last glacial maximum
Lacustrine
Orbital forcing

ABSTRACT

We employed a new, multi-proxy record from Baldwin Lake (~125–10 ka) to examine drivers of terrestrial Southern California climate over long timescales. Correlated bulk organic and biogenic silica proxy data demonstrated high-amplitude changes from 125 to 71 ka, suggesting that summer insolation directly influenced lake productivity during MIS 5. From 60 to 57 ka, hydrologic state changes and events occurred in California and the U.S. Southwest, though the pattern of response varied geographically. Intermediate, less variable levels of winter and summer insolation followed during MIS 3 (57–29 ka), which likely maintained moist conditions in Southern California that were punctuated with smaller-order, millennial-scale events. These Dansgaard-Oeschger events brought enhanced surface temperatures (SSTs) to the eastern Pacific margin, and aridity to sensitive terrestrial sites in the Southwest and Southern California. Low temperatures and reduced evaporation are widespread during MIS 2, though there is increasing evidence for moisture extremes in Southern California from 29 to 20 ka. Our record shows that both orbital-scale radiative forcing and rapid North Atlantic temperature perturbations were likely influences on Southern California climate prior to the last glacial. However, these forcings produced a hydroclimatic response throughout California and the U.S. Southwest that was geographically complex. This work highlights that it is especially urgent to improve our understanding of the response to rapid climatic change in these regions. Enhanced temperature and aridity are projected for the rest of the 21st century, which will place stress on water resources.

1. Introduction

Throughout the U.S. Southwest, Great Basin, and California, climate model projections for the 21st century indicate that increased radiative forcing that will produce enhanced temperatures, aridity, and climate variability (Overpeck et al., 2013). These projections prompted our investigation of regional sensitivity to past climate change and potential forcing mechanisms over the past 125 ka, in a sector of the U.S. that is already water-stressed and increasingly populous (Georgescu et al., 2012). Retrospective studies are crucial for deepening our understanding of large-scale climate dynamics and teleconnections, and assessing the potential range of temperature and hydrological variability. Long-lasting droughts in the West during the Late Quaternary have been documented (e.g. Brunelle and Anderson, 2003; Heusser et al., 2015; MacDonald and Case, 2005; Mensing et al., 2013), most of which were associated with warm intervals (Woodhouse et al., 2010). Conversely, extreme wet events were also a feature of West Coast climates (e.g. Bird and Kirby, 2006; Kirby et al., 2013, 2012). These prolonged hydroclimatic events, on the order of

* Corresponding author.
E-mail address: kcglover@ucla.edu (K.C. Glover).

http://dx.doi.org/10.1016/j.quascirev.2017.04.028
0277-3791/

several decades or centuries, have no analogue in the past 150 years of instrumental records.

A growing body of climatic records from the U.S. Southwest, Great Basin, and Southern California suggests regional sensitivity to a variety of climate drivers that include an atmospheric-oceanic teleconnection with the North Atlantic (Asmerom et al., 2010; MacDonald et al., 2008; Oster et al., 2014; Reheis et al., 2015; Wagner et al., 2010), Pacific Ocean (Hendy and Kennett, 2000a; Heusser, 1998; Lund and Mix, 1998) boreal insolation (Lachniet et al., 2014; Moseley et al., 2016), and migrating storm tracks (Garcia et al., 2014; Kirby et al., 2006; Owen et al., 2003). Offshore marine cores have documented long histories through several Marine Isotope Stages (MISs), but with dynamically different responses compared to terrestrial sites (Heusser and Basalm, 1977; Hooghiemstra et al., 2006). The longer-term climate history of terrestrial Southern California throughout past glaciations and multiple MISs is lesser-known, compared to abundant studies on the Holocene and last glacial (MIS 2).

In this study, a newly-acquired core from Baldwin Lake in the San Bernardino Mountains (SBM) that spanned 125 to 10 ka provided insight to the long-term temperature and hydrological variability of Southern California, and associated climatic drivers. We use this material to address the following questions: Is alpine Southern California sensitive to orbital and North Atlantic forcing over long timescales? How does the record of paleoenvironmental change and climatic variability at Baldwin Lake compare to other Southern California, Great Basin and Southwestern sites over the past 125 to 10 ka?

2. Setting

Located east of the Los Angeles Basin, the SBM are part of the Transverse Ranges and include some of the highest elevation peaks in Southern California. The SBM form a barrier between the interior Mojave and Sonoran Deserts, and the summer-dry, winter-wet Mediterranean conditions towards the coast. The San Andreas and Mill Creek Faults bound either side of the SBM range. Triassic-to Cretaceous-age granitic rocks dominate the SBM range (Morton and Miller, 2006), with other allocthonous sedimentary terranes of Precambrian and Mesozoic age (Dibblee, 1964). High relief valleys and slopes are often covered with Quaternary deposits, including alluvium, talus, and fanglomerates.

Baldwin Lake (34.275°N, 116.8°W) lies at an elevation of 2060 m in the Big Bear Valley of the SBM, approximately 160 km east of the Pacific coastline (Fig. 1). It is presently an intermittent lake, and one of two major lake basins in Big Bear Valley, with a 79 km^2 watershed (Big Bear Lake TMDL Task Force, 2012). To the west, the Big Bear Lake watershed is 96 km^2, and supported a lake throughout the Holocene (Kirby et al., 2012; Paladino, 2008). Sugarloaf Mountain to the south (3033 m) is the primary sediment source of the Baldwin basin, via the 14 km^2 Sugarloaf fan (Flint and Martin, 2012; Leidy, 2006). Smaller-scale faults occur throughout Big Bear Valley, including a thrust fault <1 km east of Baldwin Lake on Nelson Ridge (Flint and Martin, 2012). The highest elevations of the Transverse Ranges were glaciated during MIS 2; moraines still persist on the northern flank of Mt. San Gorgonio (3506 masl) and mark later Holocene readvances (Owen et al., 2003).

Mediterranean winter-wet and summer-dry conditions prevail throughout the SBM and Southern California, modulated by upwelling and currents on the North American Pacific margin. The configuration of the North Pacific High and North American Low, and westerly winds, drive this strong precipitation seasonality (Barron et al., 2003; Cayan and Peterson, 1989). Seasonal migration of the Polar Jet Stream (PJS) brings Pacific-derived moisture in the winter months, and Southern California's yearly precipitation averages 13–64 cm at lower elevations, and 64–150 cm in the mountains (National Oceanic and Atmospheric Administration, n.d.). Annual precipitation averages are comparatively higher in Big Bear Valley, averaging ~220 cm/yr (U.S. Climate Data, 2016) and the moisture is largely derived from North Pacific winter storms (Wise, 2010). Other precipitation sources include orographic uplift, lateral snow drift (Minnich, 1984), and occasional summer storms that result from convection or dissipating tropical cyclones (Tubbs, 1972). Average July high temperature at Big Bear City is 27.2 °C, and January's average high is 8.3 °C (U.S. Climate Data, 2016).

3. Materials and methods

3.1. Core recovery and Initial Core Description (ICD)

We re-cored Baldwin Lake in August 2012 at the basin depocenter (34°16.56633′, −116°48.61182′) with a CME-95 truck-mounted hollow stem auger drill. Prior coring at Baldwin Lake in 2004 yielded a 14.2 m sequence referred to as BLDC04-2 (Fig. 1; Kirby et al., 2006). We refer to the new sequence of cores as BDL12, which consisted of overlapping 2.5 foot sections from two separate holes totaling 27 m, now archived at UCLA. Cores were split at UCLA in 2013, then photographed and described at University of Minnesota's Limnological Research Center (LRC) in 2014, following conventions for Initial Core Description (ICD; Schnurrenberger et al., 2003). Key sedimentary structures and changes, described by depth from surface, have been summarized for the Supplemental Information.

3.2. Sedimentary analyses

Initial magnetic susceptibility (MS) data were collected at UCLA with a Bartington MS2e sensor, and later replicated at LRC. The GeoTek Multi-Sensor Core Logger at LRC collected 0.5-cm interval data. Loss-on-ignition (LOI) analysis at 1-cm intervals throughout BDL12 determined the bulk organic and carbonate content of the sediment (Dean, 1974; Heiri et al., 2001). Organic content was determined from the mass lost from1-cm^3 volume samples after 1-h burns at 550 °C in a muffle furnace, and carbonate content was calculated after subsequent 1-h burns at 950 °C. Core density was calculated from sample dry weight values recorded during LOI analysis. Bulk inorganic values were percentage values, calculated from the remaining sample weight after all LOI burns compared to the initial dry weight. Mass accumulation rates (MARs) were calculated by multiplying a horizon's dry density by the sedimentation rate derived from the age model (Rack et al., 1995). The 1-cm LOI and MS data were used to correlate the core sections, and determine a depth-below-surface value for each horizon of the sequence.

Grain size sampling was initially done at 50 cm intervals (Silveira, 2014), with later sampling that targeted the basal coarse-grained facies, and the slowly-deposited MIS 2 interval. Samples (n = 93) were digested in 30–35% H_2O_2 to remove organics, then 1N HCl to remove carbonates, and lastly 1M NaOH to remove biogenic silicates, with intermittent centrifuging. Analyses were performed on a Malvern Mastersizer 2000 laser diffraction grain size analyzer at California State University – Fullerton. The results were combined with high-resolution grain-size data from core BLDC04 (Blazevic et al., 2009) after re-aligning BLDC04's measured depths to correlate with BDL12 (see Supplemental Data). We reported the grain size mode (i.e., most frequently-occurring size) here in μm, after averaging values at 25-cm intervals for the core above 15 m, and at 50-cm intervals for the core section spanning 15–27 m. This was done to reduce noise and variable sampling resolutions throughout the ~27 m sequence. X-ray fluorescence

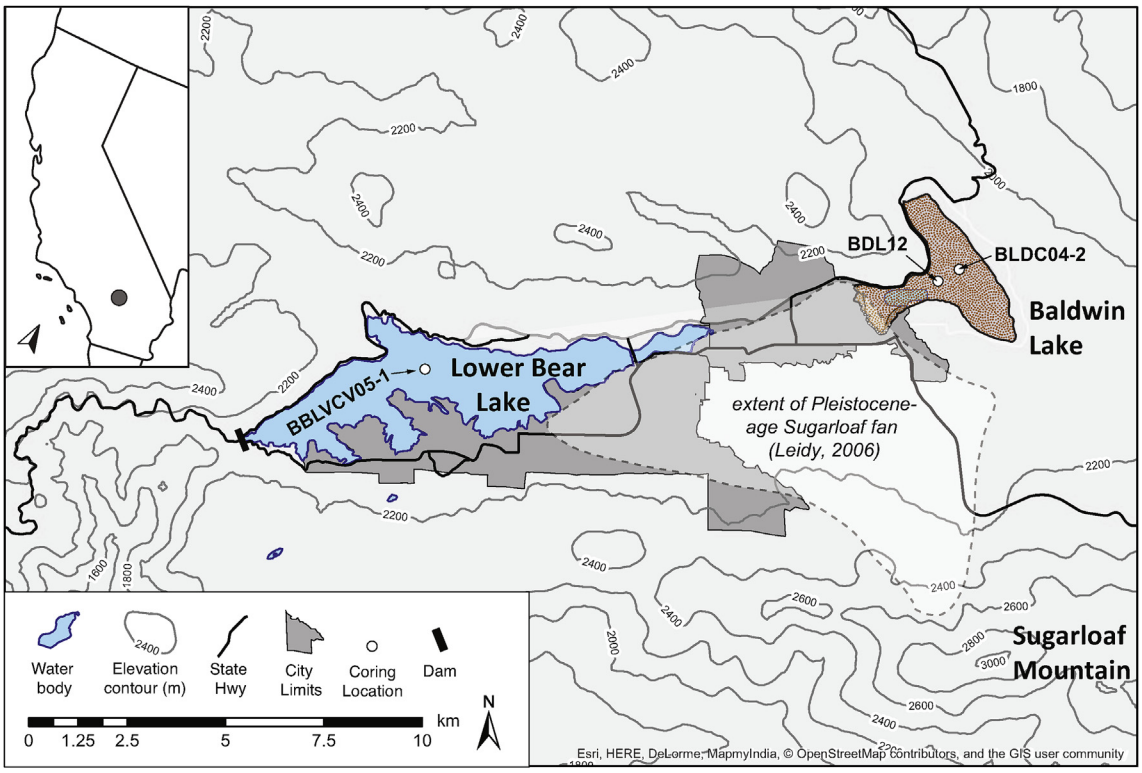

Fig. 1. Map of Big Bear Valley, San Bernardino Mountains, California. Cores taken in include Lower Bear Lake (BBLVCV05-1; Kirby et al., 2012), Baldwin Lake (BDLC04-2; Kirby et al., 2006; Blazevic et al., 2009) and a second core from Baldwin Lake (BDL12; this study). Contour interval = 200 m.

(XRF) values were taken with a portable Innov-X Analyzer at 5 cm intervals along a split core surface that was lined with Ultralene film. Elements reported here include titanium (Ti), iron (Fe), calcium (Ca), potassium (K), and manganese (Mn).

3.3. Biogenic Silica (BSi)

We selectively analyzed biogenic silica (BSi) throughout the core in order to determine if lake productivity was a primary contributor to organic content changes. Amorphous silica is a structural component of diatoms, radiolarians, sponges, and phytoliths in aquatic environments. Its measurement can potentially establish paleoproductivity and radiative influence in long lake histories (e.g. Prokopenko et al., 2006; Wohlfarth et al., 2008). Samples (n = 32) from each of the Marine Isotope Stages were analyzed with wet-alkaline extraction (Conley and Schelske, 2002) to characterize the relationship between organic content and BSi in different core facies.

3.4. Chronologic control – assumptions and approach

We present a new age model here that extends to Marine Isotope Stage 5, and replaces the chronology of Kirby et al. (2006). The prior BLDC04-2 chronology included bulk dates that were not securely cross-dated with other methods, such as macrofossils or tephra layers (Zimmerman and Myrbo, 2015). From BDL12, AMS ^{14}C dating was conducted on seven wood and charcoal samples from the upper 8 m (Table 1). Infrared Stimulated Luminescence (IRSL) single-grain analysis was conducted on lower sections of the sequence that possessed a higher sand fraction (Buylaert et al., 2009; Rhodes, 2015). IRSL was applied to 150–175 μm K-feldspar grains, a technique increasingly used in sites from Southern California, where quartz demonstrates low sensitivity in many locations (Garcia et al., 2014; Lawson et al., 2012). Four 20-cm sections of core were removed with a handsaw under luminescence laboratory lighting conditions, and a ~1.5 cm diameter cylinder of sediment was extracted from the core interior for IRSL dating. Once disturbed, these sections were not further analyzed. Preparation procedures, measurement at UCLA, and analysis followed Rhodes (2015). Fading measurements were used to correct both the IRSL signal measured at 50 °C and the post-IR IRSL signal at 225 °C, which demonstrated mean g-values of 0.03 and 0.015 respectively. Dose rates were calculated using ICP-MS (for U, Th) and ICP-OES (for K) determinations at SGS, Vancouver, Canada.

In order to construct the age model, we hypothesized that lake productivity was the primary contributor to total organic deposition, and responded to changes in radiation. This was based upon establishing relationships between key proxies, and making certain assumptions about basin response from the available data. First, we determined that total organic matter and BSi data were correlated to each other ($r = 0.81$, $p < 0.001$) throughout the basin's history. This suggests that primary productivity, rather than preservation, was a key contributor to organic matter variation (Colman et al., 1995; Conley and Schelske, 2002; Kaplan et al., 2002). Second, we hold that local radiation is an important control on the length of the freshwater photosynthetic season (e.g. Colman et al., 1995; Hu et al., 2003) and seasonal ice cover of the lake surface (McKay et al., 2008; Melles et al., 2006; Prokopenko et al., 2006). This assumption underlies our use of relatively local (30°N) summer insolation values as a proxy for seasonal light intensity, and primary driver for the associated peaks and troughs in total organic matter. This relationship between 30°N summer insolation and organic deposition was initially proposed for the site in the BLDC04-2 study (Kirby et al., 2006). The new organic matter dataset presented here replicated this apparent correlation to 30°N insolation in a 20-kyr section of core constrained with radiocarbon dating (40–20 ka).

Table 1
AMS radiocarbon dates, infrared-stimulated luminescence dates, and tie points used for BDL12's age model. Mean age from Bacon 2.2 (based upon IntCal13; Reimer, 2013) is used for the calendar-years age model; see text and Fig. 2 for details.

Accelerated Mass Spectometry Radiocarbon Dates *W. M. Keck Carbon Cycle AMS Radiocarbon Lab, UC-Irvine*				
Sample No.	Depth (cm)	Material	Raw ^{14}C Age	Approximate Calendar Age
UCI-121791	152	charcoal	10,010 ± 320	~11,868
UCI-124533	262	charcoal	21,150 ± 810	~24,307
UCI-124534	389	charcoal	25,170 ± 280	~29,339
UCI-121792	440	pine cone piece	25,990 ± 140	~30,400
UCI-124535	529	charcoal	27,240 ± 180	~31,474
UCI-124536	745	charcoal	35,710 ± 790	~40,417
UCI-121793	815	twig	41,010 ± 700	~43,997
Post-IR Infrared Stimulated Luminescence dates *Earth and Planetary Sciences Dept., UCLA*				
Sample No.	Depth (cm)	Material	50°C IRSL Signal (cal yr BP)	225°C IRSL Signal (cal yr BP)
J0395	2075	massive silt	88,500 ± 6200	87,800 ± 6100
J0396	2173	clayey silt	55,800 ± 5400	44,900 ± 3900
J0397	2570	sand	117,000 ± 8000	109,000 ± 8000
J0398	2700	sand	136,000 ± 10,000	124,000 ± 8000
Tie-Points for orbital tuning				
	Depth (cm)			Age (cal yr BP)
	1573			71,000
	1746			83,000
	2060			94,000
	2197			105,000
	2433			116,000

Visual curve matching (Groot et al., 2014) is a technique often used in the absence of other chronologic data or techniques (e.g. Tzedakis et al., 2001), or to supplement existing dates (e.g. Cacho et al., 1999). We employed it here it as a first-pass interpretation of basin response to climate drivers, and to construct a working age model for the newly-recovered long paleorecord. A series of tie points that match five peaks and troughs in the insolation and bulk organics datasets were established during MIS 5 (~116–71 ka; Table 1; Fig. 2b). This exercise assumes that basin response to insolation shifts was immediate. While highly-resolved, directly-dated speleothem records spanning MIS 6–1 showed that Great Basin paleotemperature response lagged boreal insolation shifts by ~3 kyr (Lachniet et al., 2014), there is not yet evidence for a similar lag at California sites. Age uncertainties from recent California paleorecords are comparatively greater (e.g. Herbert et al., 2001; Kirby et al., 2015; Oster and Kelley, 2016; *this study*). We ascribed

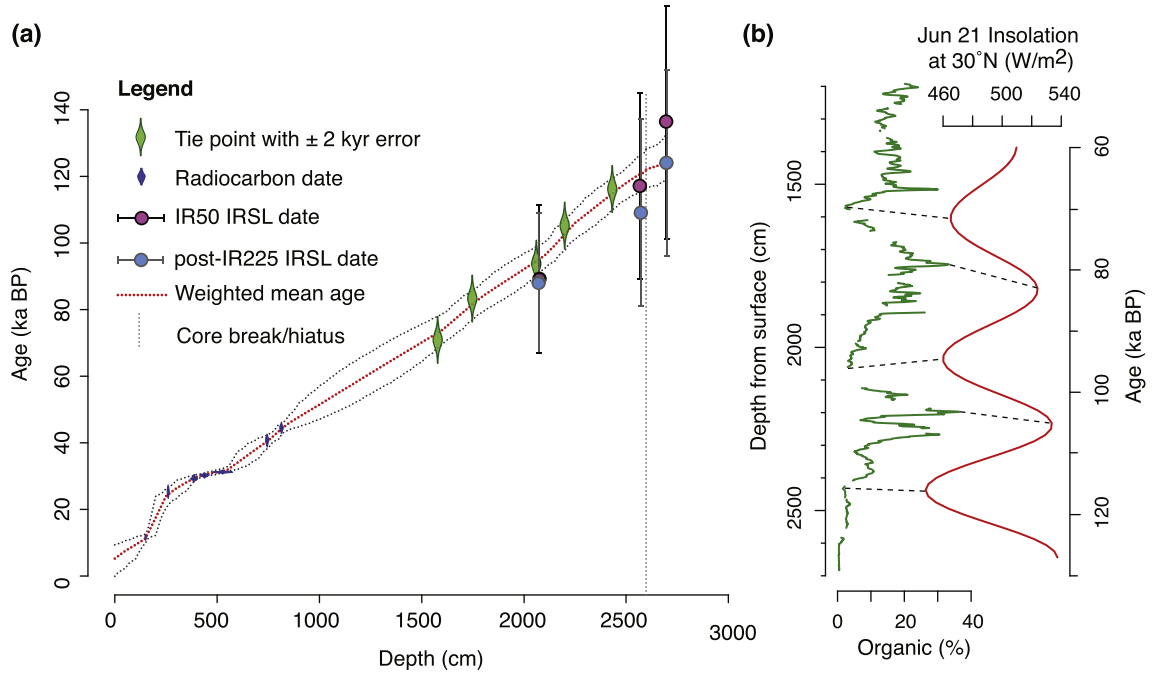

Fig. 2. a) Bacon 2.2 age-depth model from radiocarbon dates, luminescence dates, and tie-points (Table 1). b) Tie-points established between insolation peaks and troughs from summer values at 30°N (Laskar et al., 2004), and corresponding maxima and minima in a 5-point moving average of high-resolution organic content data throughout BDL12.

a 2-kyr uncertainty to each tie-point for the Bacon 2.2 model (e.g. Mahan et al., 2014). This allowed for the possibility of 1) leads/lags in lake response compared to insolation, 2) influences other than temperature on organic matter production (e.g. nutrient cycling, moisture variability, and lake level variability), and 3) horizons where the tie-points overlapped with IRSL dates.

Bacon 2.2 is a Bayesian approach to modeling the age of terrestrial cores (Blaauw and Christen, 2011), and was employed for our age-depth model, incorporating ^{14}C dates, 50 °C and post-IR 225 °C luminescence dates, and five tie-points (Table 1, Fig. 2). Bacon 2.2 algorithms perform calendar year conversions on ^{14}C dates using IntCal13 (Reimer, 2013), and incorporate 2-sigma results in the model. In our model, the sediment mean accumulation rates was set to 50 cm/yr, and core section thickness was 50 cm, both suggested by the program (Blaauw and Christen, 2011). Default priors for memory strength and memory mean (i.e., the degree to which sedimentation rate depends on that of adjacent horizons) were retained (Blaauw and Christen, 2011; Goring et al., 2012). Luminescence sample J3096 was excluded, as it had low yield, displayed non-standard TL during preheat measurements, and was not in stratigraphic agreement with the other three samples (Table 1). A sharp break between clayey silt and the basal coarse-grained sandy layer downsection occurred at 2596 cm, possibly indicating of a hiatus. The uppermost lake sediments above 152 cm, where the youngest radiocarbon date was obtained, have an uncertain age. Bacon 2.2 thus extrapolated the model between 0 and 152 cm without constraints.

4. Results and proxy interpretation

4.1. Age model

The weighted mean ages from the Bacon 2.2 age model (Fig. 2) ranged from 125.7 to 5.3 ka cal BP, and were used for plotting figures, and the ensuing discussion of regional paleoclimate events. Without reliable age control above 152 cm, we were not confident that the Middle Holocene was the true age of the core top, and have excluded the desiccated upper 1 m of BDL12 from the ensuing figures and discussion. Direct dating of a charcoal fragment yielded a date of ~11.9 ka, and was obtained from a 3-cm charcoal layer (154-151 cm) not captured in the BLDC04-2 core. Previously, the upper material in the basin had been constrained by a ~20.3 ka bulk date at 114–117 cm (Kirby et al., 2006). Our new series of ^{14}C dates suggested, instead, that basin deposition continued after the Last Glacial Maximum (LGM) and included the Pleistocene-Holocene transition, though at very slow sedimentation rates (<0.03 cm/yr). The fading-corrected IRSL ages measured at 50 °C and post-IR IRSL at 225 °C were within range of the tie-points established (Table 1, Fig. 2). The Bacon 2.2 age model (Fig. 2), however, produced ages at the tie-point horizons that were 0.6–2.5 kyr offset from the ages initially assigned (Table 1). This was the result of assigning each a ±2 kyr error, and the influence of the IRSL dates in the model.

4.2. Sedimentology and Summary of proxy data

The BDL12 sequence was 91.9% complete, with some missing portions due to coring gaps and disturbances. Details of core stratigraphy are described by depth and approximate age in the Supplemental Information. Key changes in core stratigraphy and sedimentological data (dry density, inorganics, MARs, and grain size) are shown by depth in Fig. 3. Grain size mode results throughout the sequence were consistently in the range of silt (2–50 μm), except for the basal sand unit (mode >400 μm). We summarized important sedimentological changes, as related to density and grain size, in Table 2 with the modifiers “sandy,” or “clayey” for cases when these size fractions were ≥20%, and the silt remained the dominant fraction (≥60%). Fig. 4 shows proxy data by age and MIS, with 30°N summer insolation shifts. MIS 5 substages are referenced with letters (e.g. MIS 5a), though age boundaries between substages have no global standard, and tend to vary geographically (Imbrie et al., 1984).

4.3. Relationships and environmental interpretation for Baldwin Lake proxy data

We assumed the following relationships between proxy data, environmental conditions, and local summer insolation in our interpretation of site history. The immediate response for primary productivity to 30°N summer insolation during MIS 5 and MIS 3/2 was discussed in detail in section 3.4, as this assumption underpinned the age model. For Baldwin Lake, we interpreted positive correlation between BSi and total organic content as evidence that paleoproductivity was the dominant control on organic deposition. Several factors could have influenced the large changes observed in the coupled organic-BSi proxy data throughout the record. Correlated organic-BSi data have indicated shifts in lake water temperature at other high latitude or altitude sites (e.g. Blass et al., 2007; Hahn et al., 2013; McKay et al., 2008; Nussbaumer et al., 2011; Street et al., 2012; Vogel et al., 2013). High concentrations of BSi may also be linked to periods of increased runoff, and nutrients, within catchments (Ampel et al., 2008; Conley and Schelske, 2002). Organic deposition as a proxy for relative wetness in the SBM has also been suggested, with 30°N summer insolation impacting precipitation dynamics and moisture delivery to Southern California (Kirby et al., 2006). While it is challenging to disentagle how much each of these processes contributed to bulk organic measurements over time, key periods when one process seemed most dominant are discussed in the paleoenvironmental history of the basin below (section 5.1), with supporting evidence.

Times of high organic deposition generally coincided with low values of both magnetic susceptibility and dry density (Table 2). Low MS values (<12 SI) throughout most of BDL12 (Fig. 4, Table 2) suggest this proxy detected a largely diamagnetic fraction throughout basin history (Dearing, 1999). Bedrock sources are largely granodioritic, yet the MS signal was dampened at times of episodic, high-energy clastic input. We hypothesized that in this basin, sediment frequently underwent sulfide reduction at the lake bottom, particularly when the lake was productive and organic deposition was ≥10%). Such a reduction process can partially or completely dissolve magnetite, and produce low MS values (Dearing, 1999; Kirby et al., 2007; Nowaczyk et al., 2006).

Trace element data aided our interpretation of allochthonous deposition, lake level changes, and lake ventilation. We interpreted relatively higher values of Ti, and in part, Fe, to phases of increased detrital, non-biogenic sediment deposition (Kylander et al., 2011; Vogel et al., 2013). Ca values changed in tandem with and were highly correlated to $CaCO_3$ ($r = 0.84$; Fig. 4h–i), suggesting that trace element Ca was largely derived from the precipitation of $CaCO_3$, rather than bedrock sources in the watershed. Such calcite precipitation tends to occur in lake systems when warm water temperatures, and potentially lake regression, produce saturation, leading to high $CaCO_3$ values (Hodell et al., 1998). High values in the manganese to titanium ratio (Mn:Ti; Fig. 4) have been interpreted as a proxy for a well-mixed lake with bottom ventilation (Kylander et al., 2011). Times of high Ca, $CaCO_3$ and Mn:Ti, including 114–107 ka, 87–75 ka, and 14–10 ka (Fig. 4), and were distinct facies, with lighter gray-brown sediment and, from 87 to 75 ka, horizons with mollusk shells. We interpreted the combination of increased Ca, $CaCO_3$, and Mn:Ti to indicate phases when Baldwin Lake was

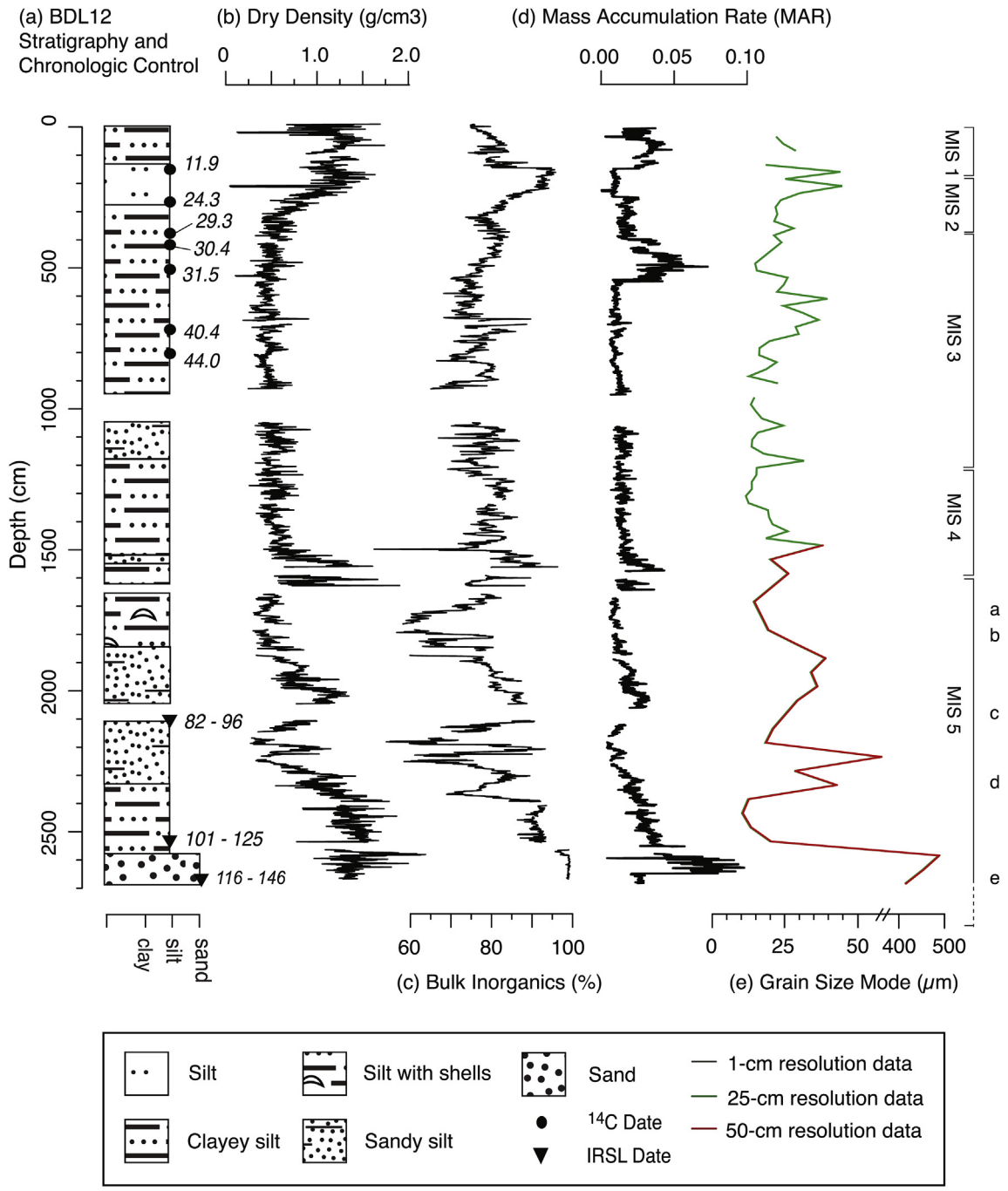

Fig. 3. Stratigraphy, age horizons, and sedimentological data for BDL12, with approximate boundaries of Marine Isotope Stages after Lisiecki and Raymo (2005). The age range for three pairs of post-IR IRSL dates are shown. Substage lettering (MIS 5e – 5a) is not bracketed at specific time points, due to this age uncertainty.

warmer and well-ventilated. This warming may have also resulted from the lake shallowing. At horizons when all three of these parameters remained low, we assumed a stratified lake. When such conditions are coupled with high productivity, the deposition and bacterial decomposition of phytoplankton could produce reducing conditions and an anoxic lake bottom, and thus removal of a strong magnetic signal (Dearing, 1999).

5. Discussion

5.1. Baldwin Lake's environmental change from 125 to 10 ka

The basal luminescence age results at 2700 cm depth, with potential dates of 136 ± 10 ka (50 °C IRSL signal) or 124 ± 8 ka (225 °C IRSL signal; Table 1), suggested that deposition of the BDL12 sequence began during MIS 5e. This facies was largely comprised of dense, coarse, massive sand. With <1% fine grains, we interpreted these basal sediments to be well-winnowed, and deposited under high-energy conditions. Fluvial and colluvial processes likely dominated erosion and transport in the alpine valley at this time, with the Baldwin Basin possibly connected to adjacent Lower Bear Basin (Fig. 1). The transition to finer-grained clayey silt was abrupt and interpreted as a hiatus, largely because IRSL-dated results from either side of the break have a difference of ≥10 kyr over 1.3 m of core. Rapid sedimentation from Sugarloaf Mountain, including possible landslide events (e.g. the Sugarloaf Fan; Fig. 1), may have

Table 2
Multi-proxy summary from Baldwin Lake core BDL12, by Marine Isotope Stage (MIS). MS = magnetic susceptibility, reported in SI units (10^5 of measured values). $CaCO_3$ = carbonate content from loss-on-ignition analysis. Trace element data (Ca, Fe, Ti, and Mn:Ti) reported as average ppm for each MIS, unless otherwise noted. "Insolation" refers to summer insolation at 30°N (Laskar et al., 2004), except for MIS 3, where both summer and winter are noted. For MIS 5, substages with letters (e.g. MIS 5b) refer to the span of the entire substage and its conditions, and are ordered alphabetically youngest-to-oldest.

Stage/Substages Cal Yr BP	Key Changes in Insolation and Proxy Data	Key Paleoenvironmental Conditions/Events
MIS 5e (125–120)	• relatively rapid insolation shift from 528 W/m^2 at 127 ka, to 474 W/m^2 at 120 ka • sand facies throughout (grain size mode >400 μm); minimal clay (<1%) • high dry density (>1.2 g/cm^3), MS < 7 SI throughout; average value 3.2 SI • Ti (~2400 ppm) and Fe (~8500 ppm) low until rapid increase to 3500 ppm (Ti) and >20,000 ppm (Fe) at 121 ka • low organic content (<1%), $CaCO_3$ (<3%) and Ca (~6800 ppm) throughout; no BSi analysis	• High-energy deposition
MIS 5d – 5c (120–95)	• insolation low 448 W/m^2 at 116 ka, rose to 533 W/m^2 by 105 ka, declined to 460 W/m^2 by 95 ka • fine-grained, inorganic clayey silt throughout, with fine sand (grain size mode = 58 μm) at 106 ka • MS rose from ~7 SI to ~16 SI from 121 to 118 ka, gradually declined to <5 SI by 112 ka, generally stayed below <6 SI until 95 ka, except for short excursion at 101 ka (51 SI) • high Ti (~3500 ppm) and Fe (~35,000 ppm) until 112 ka, lows of ~600 ppm (Ti) and ~8000 ppm (Fe) at 107 and 102 ka, moderate-to-high Ti (~2500 ppm) and Fe (~25,000 ppm) began 98 ka • low-to-moderate Ca (~20,000 ppm) and $CaCO_3$ (5000–10,000 ppm) until peak at 112 ka (Ca ~109,000 ppm, $CaCO_3$ ~20%), then declined over next 8 kyr until 95 ka • low organics (<5%) until 113 ka, peaks ~33–39% at 106 ka and 103 ka, declined to <5% by 95 ka • BSi generally followed organics, with 1–3 mg/g background, peak of 11.3 mg/g at 103 ka	• Basin closure near onset of MIS 5d • Cool, deep, unproductive lake conditions ascribed to MIS 5d insolation minimum • High-erosion event 106 ka • Transition to more shallow, productive lake late MIS 5d; peak productivity during MIS 5c (103 ka)
MIS 5b – 5a (95–71)	• insolation rose from 460 W/m^2 at 95 ka to 524 W/m^2 by 83 ka; declined to 465 W/m^2 by 72–71 ka • silt deposition throughout, with calcareous layers including mollusks that end abruptly 81 ka • MS low (<2 SI) between 86 and 76 ka; rose to 5–7 SI by end of MIS 5 • moderate Ti (~1200 ppm) and Fe (17,000 ppm) at 95 ka, declined to <100 ppm and ~6000 ppm by 83 ka, gradually increased to 1700 ppm and 18,000 ppm by 71 ka. • moderate Ca (25,000–60,000 ppm) until 89 ka, then maxima 180,000 ppm at 86 ka, and 160,000 ppm at 83 ka. $CaCO_3$ ranged 5–15%, with peaks 22% at 86 ka, and 30% at 83 ka. Mn:Ti 0.84 at 83 ka and 0.74 c. 86 ka. • varied organic content: minima are <5% from 95 to 93 ka and 73–72.6 ka, maxima of ~33% at 88.2 ka and 81.6 ka. Maximum for BDL12 is 44% at the MIS 5a/MIS 4 transition (71 ka) • BSi varied with organics, with peak value 17.4 mg/g at 82.6 ka	• High-amplitude change in lake productivity • Lowstand conditions evident at 87 ka and 82 ka, with abrupt transition out of the latter, likely due to rapid shift in available moisture
MIS 4 (71–57)	• low insolation 465 W/m^2 at 71 ka increased to 510 W/m^2 by 60 ka • clayey silt (density ~0.70 g/cm^3) deposition that transitioned to organic silt (density <0.54 g/cm^3) • moderate-to-high organics (average = 16.5%); BSi at late MIS 4 (55–51 ka) was 9.8–11.5 mg/g • moderate-to-low MS, Ti and Fe throughout (MS ~5.0 SI, Ti ~1500 ppm, Fe ~20,000 ppm) • shallow-water indicators were moderate at onset of MIS 4: Ca (22,000 ppm), $CaCO_3$ (<11%), but decline by 69 ka and remain low (Ca ~4900 ppm, $CaCO_3$ <5%, Mn:Ti ~0.11),	• Basin shift occurred 69 ka towards deeper lake and sustained productivity that persisted after MIS 4
MIS 3 (57–29)	• summer insolation ranged between 481 and 506 W/m^2; winter insolation 213–227 W/m^2 and maintained 220 W/m^2 from 49 to 37 ka • fine-grained organic silt (mode 12–39 μm), dry density <1.00 g/cm^3 (average = 0.48 g/cm^3) • low MS (average = 3.9 SI); Ti decreased from ~1700 to 900 ppm by 37 ka, then increased to ~1400 ppm by 29 ka. Broad decrease and increase in Fe (ranged ~11,000–21,000 ppm) with shorter, rapid increases throughout (~51,000 ppm) • suppressed Ca (~2500 ppm) and $CaCO_3$ (<10%, average of ~4.3%) throughout MIS 3 • moderate organic content (average = 18.8%), with millennial-scale fluctuations ranging 10–28%	• lowest-amplitude variation in both summer and winter insolation for nearly 30 kyr; reduced seasonality • Consistently productive lake that remained stratified and deep • Organic content does not shift in tandem with summer insolation, and millennial-scale fluctuations suggest North Atlantic forcing (Fig. 5)

(*continued on next page*)

Table 2 (*continued*)

Stage/Substages Cal Yr BP	Key Changes in Insolation and Proxy Data	Key Paleoenvironmental Conditions/Events
MIS 2 (29–14)	• BSi relatively high throughout MIS 3, ranging 7.7–13.4 mg/g • insolation low of 471 W/m^2 at 23 ka, reached 509 W/m^2 by 14 ka • predominantly silt deposition, with a coarser layer (28% sand) 28 ka; deposition rate declined by more than half (~0.05 cm/yr during MIS 3 to ~0.02 cm/yr for MIS 2 m) • MS maximum at LGM start, with peak at 26 ka (~100 SI) above background values of 0–11 SI • high Ti (2300–3600 ppm) and Fe (average 26,000 ppm, with 56,000 ppm peak) began 26.3 ka, maintained until MIS 1 • low Ca (6000 ppm), $CaCO_3$ (generally <5%) and Mn:Ti (0.12) throughout • final organic content increase to 23% at 27.7 ka, then decline to <5% by 21 ka and thereafter • BSi decreased overall from 7.9 to 5.4 mg/g, though with peaks and lags separate from organics. *Pediastrum* are abundant 24 ka, and trace element phosphorus began increase 27 ka from ~7000 ppm, reaching ~14,000 ppm by 14.5 ka	• Low insolation, cold conditions, and deep water • last phase of moderate productivity at 27.7 ka not paced with insolation • BSi suggests moderate-to-low lake productivity during MIS 2, perhaps due to high K influx and abundant *Pediastrum* 24 ka
MIS 1 (<14)	• insolation continued its increase to 515 W/m^2 by 11 ka, declined to 488 W/m^2 by 5 ka • desiccated, inorganic clayey silt (mode grain size <29 μm); dry density is high (0.67–1.74 g/cm^3) • erratic MS, varying between −2.6 - 8 SI; high Ca (~84,000 ppm), low Ti (~1300 ppm), generally low Fe (18,000 ppm) with excursion ~73,000 ppm at 11.8 ka, high Mn:Ti (0.58) • relatively high carbonate content; abrupt rise at 12.7 ka to ~15%; MIS 1 average 14.6% • low organic content (<10%, average 4.7%) and two moderate BSi horizons (4.5–7.8 mg/g)	• Transition to intermittent lake • Desiccation, low sedimentation, and uncertain age prevent study of lake conditions after c. 10 ka

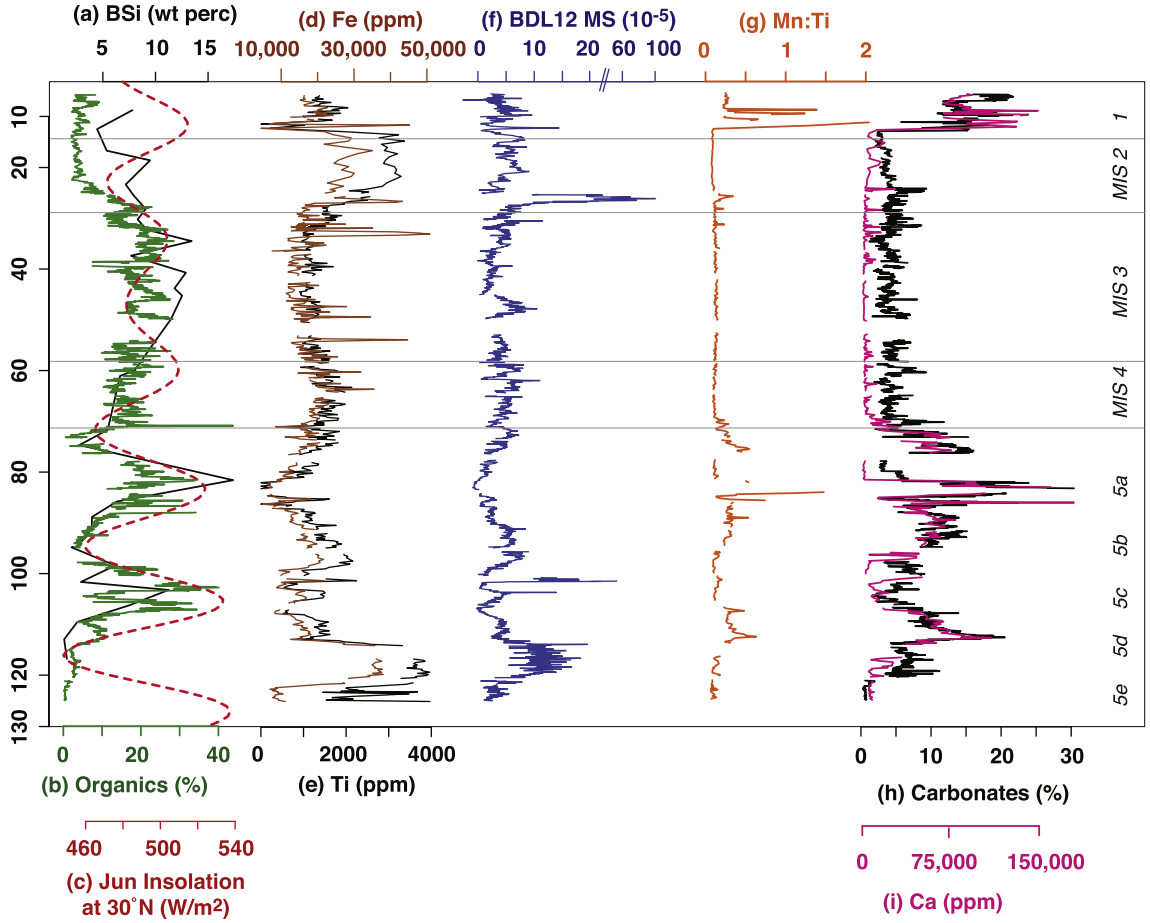

Fig. 4. Physical and geochemical data, plotted by age and with Marine Isotope Stage boundaries noted. (a) Biogenic silica. (b) Bulk organic content, determined with loss-on-ignition. (c) Summer insolation at 30°N. (d) Trace element iron (Fe). (e) Trace element titanium (Ti). (f) BDL12 magnetic susceptibility (SI). (g) Manganese to titanium ratio (Mn:Ti). (h) Bulk carbonate content ($CaCO_3$), determined with loss-on-ignition. (i) Trace element calcium (Ca).

aided closure of the basin, and the separation of the Baldwin and Lower Bear Lake basins (Leidy, 2006; Stout, 1976).

Trace elements that were key to the interpretation of MIS 5e conditions are reported in Table 2 with approximate values. Sediment upsection of the basal sand possessed high Ti and Fe, and low carbonate and organic content (Table 2, Fig. 4). This largely detrital, inorganic deposition suggests that Baldwin Lake remained deep, unproductive, and cool for the first half of MIS 5d during a summer insolation minimum at 116 ka. Ca, $CaCO_3$, and organics later increased at 112 ka while MS decreased, indicating the lake became warmer, shallower, and more productive.

The period centered around MIS 5c was the basin's first productive phase from 109 to 96 ka, with organic values reaching >30% on two occasions between 106 and 103 ka, and BSi of ~11.3 mg/g. Productivity declined to minimal levels by 95 ka (Table 2, Fig. 4a–b). During MIS 5b – 5a (95–71 ka), productivity again increased and decreased, reaching >30% at 83 ka. Lowstand conditions occurred during MIS 5b, with high Ca, $CaCO_3$, and Mn:Ti (Table 2, Fig. 4). Abundant littoral mollusks *Lymnaea* and *Planorbella* spp. (Burch, 1982) indicate that the lake shoreline had reached the basin depocenter, where the core was taken. All Ca-based lowstand evidence quickly disappeared at 82 ka, and organics surged to 33% by 81.6 ka in the deeper water, before declining alongside summer insolation to reach ~1% at 73 ka.

During MIS 4 and 3, lower amplitude oscillations in summer insolation apparently yielded a long-term state of lake productivity, perhaps because seasonal insolation was less variable. Organics increased from the onset of MIS 4 (71 ka), and then maintained moderate values (average = 16.4%; Fig. 4b). Early MIS 4 had relatively high levels of Ca, $CaCO_3$, and Mn:Ti (Table 2, Fig. 4g–i) that declined over the ensuing ~5–6 kyr. These lower values persisted until the end of MIS 2, suggesting lake stratification, and infrequent ventilation. Meanwhile, biologic sedimentation increased (average bulk organics = 18.8%) and underwent millennial-scale fluctuations, where bulk organic values ranged between 10 and 28%.

Periods of subtle laminae occurred during the first half of MIS 3 (57–46 ka), and are described in greater detail for core BLDC04-2 (Kirby et al., 2006). While laminated and non-laminated sediment may indicate lake water level shifts (Retelle and Child, 1996), we do not find support for the alternating perennial-to-playa conditions during MIS 3 proposed by Blazevic et al. (2009). The sediments and their chemistry are not consistent with playa conditions, best characterized by the elemental "signature" of high Ca, $CaCO_3$, and Mn:Ti that marked Baldwin Lake's desiccation at the onset of the Holocene (Fig. 4g–i). The abovementioned low concentrations of these elements persisted during MIS 3, along with low MS (Table 2, Fig. 4f), suggesting a lack of significant bottom ventilation events. These conditions lasted for most of MIS 4 and the duration of MIS 3, at least 35 kyr. This period of greater effective moisture in the SBM has also been noted in other parts of the Transverse Ranges (Santa Barbara Basin; Heusser, 1998), Valley Wells in the Mojave Desert (Pigati et al., 2011), and in the Great Basin (Maher et al., 2014).

Organic matter concentrations declined during the lower insolation and colder temperatures of MIS 2, after a final peak at 27.7 ka. Sedimentation slowed significantly and was largely detrital, with Fe and Ti increasing into the Last Glacial Maximum (LGM, 26–19 ka; Fig. 4d–e). BSi decreased to ~5 mg/g by the end of MIS 2, but moderate values (~5–10 mg/g) until that time (Table 2, Fig. 4) suggest continued productivity, despite the cold conditions and reduced light availability in the early part of this glacial. Glacial conditions can produce a sparsely-vegetated landscape and enhanced runoff capable of maintaining relatively high diatom productivity (Ampel et al., 2008), and the high Fe and Ti values suggest a similar response in the Baldwin Lake basin. The highest MS excursion in the core occurred at 27–25.5 ka; aside from oxidation of the core since its collection, there are no other unique sedimentary structures, nor shifts in other proxy data, that correspond to this excursion. One possible interpretation for this high MS peak was a decrease in reducing conditions, which would preserve the magnetic signal (Dearing, 1999).

Shallow-water indicators Ca, $CaCO_3$, and Mn:Ti increased suddenly around 12 ka, after which time Baldwin Lake likely transitioned to an intermittent, playa surface as summer insolation rose from 23 to 11 ka. Frequent dry episodes prevented further preservation of biologic material. While the Holocene is a notable omission in BDL12, a Holocene-age paleorecord from neighboring Lower Bear Lake (Fig. 1) has provided insight into SBM climate since 9.3 ka (Kirby et al., 2012).

5.2. Important climatic drivers in Southern California

5.2.1. Orbital-scale radiative forcing

California pollen sites that date to MIS 5e, including the Santa Barbara Basin (ODP 893; Heusser, 1998), ODP 1018 (Lyle et al., 2010), and Owens Lake (Woolfenden, 2003) have shown orbitally-induced landscape change. The influence of boreal summer insolation, largely credited with driving continental ice sheet mass, was a primary driver of change at interior Great Basin speleothem sites including the Leviathan, Pinnacle, and Lehman Caves (Lachniet et al., 2014), and Devil's Hole (Moseley et al., 2016). The high-amplitude shifts detected in organic matter during MIS 5 in BDL12 suggest that organic deposition was a primary response to local summer insolation, a relationship first proposed for the shorter Baldwin Lake sequence (Kirby et al., 2006).

Globally, MIS 4 conditions were milder compared to other glacials, including in the North American West and Sierra Nevada (Brook et al., 2006; Forester et al., 2005; Jiménez-Moreno et al., 2010; Phillips et al., 1996; Rood et al., 2011). At Baldwin Lake, summer insolation minima likely drove cold conditions that were short-lived, as the primary productivity increased and recovered within a few kyr of MIS 4 onset. During MIS 3, both winter and summer insolation were at their least variable in the record, reducing local seasonality (Fig. 5c). Summer insolation varied between 481 and 509 W/m^2, while winter insolation was relatively static (Fig. 5c, Table 2). This may have allowed the lake to remain ice-free, and for primary productivity to continue, for longer durations each year compared to other MISs. During MIS 2, summer insolation declined to only 471 W/m^2 (23 ka) compared to 465 W/m^2 in MIS 4, but winter insolation was slightly lower (234 W/m^2 vs. 239 W/m^2). Summer insolation reached 515 W/m^2 at 11 ka, the first time since 81 ka that radiation reached such levels. Proxy data (e.g. trace element Ca and $CaCO_3$ maxima) suggest that the lake was shallow and warm at the onset of the Holocene, a different set of conditions compared to earlier, equivalent summer insolation maxima during MIS 5 ($\geq$510 W/m^2). Enhanced evaporation and shifting precipitation are possible causes for the end of perennial conditions at Baldwin Lake, as well as the infilling of the basin (~16 m of deposition between 81 and 11 ka). After 11 ka, sediments that are massive, high-carbonate, and degraded suggest that intermittent deposition likely continued, with periods of desiccation that compromised sediment chemical and biologic preservation. Other sites in arid and semiarid California exhibited similar transitions from relatively wet towards intermittent or dry conditions at the Pleistocene-to-Holocene transition, including Owens Lake (Bacon et al., 2006) and Lake Manly/Death Valley (Li et al., 1996).

5.2.2. Millennial-scale forcing during MIS 3

We have shown that major productivity shifts in Baldwin Lake

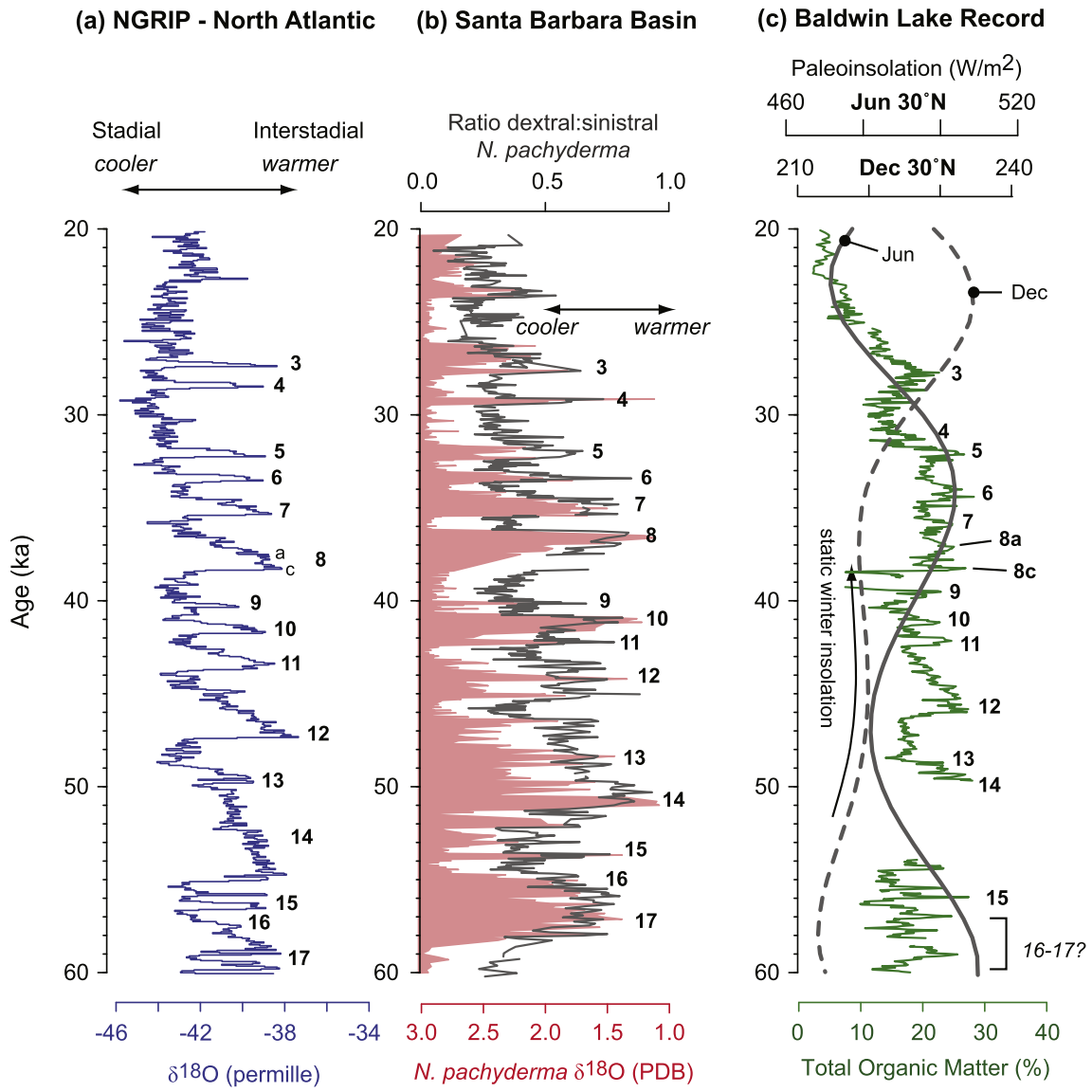

Fig. 5. (a) NGRIP $\delta^{18}O$ shifts from 60 to 20 ka, with Greenland Interstadial (GI) numbers (i.e. Dansgaard-Oschger events, Rasmussen et al., 2014). While many GIs have substages, only GI-8 has the substages shown for simplicity's sake. (b) Santa Barbara Basin core ODP-893, with interstadials labeled after Hendy and Kennett (2000a,b) and latest age model (Hendy et al., 2004). (c) Baldwin Lake core BDL12 bulk organic content from 60 to 20 ka, with summer and winter insolation (Laskar et al., 2004), and proposed D-O interstadial numbering.

likely occurred at the slow pace of orbital variation, though these changes were not without shorter-order minima and maxima, particularly during MIS 3. What rapid processes account for such change? Kirby et al. (2006) proposed these were wet events corresponding to North Atlantic interstadials, or Dansgaard-Oeschger (D-O) events. D-O events were North Atlantic millennial-scale temperature oscillations that occur between 120 and 10 ka, first recognized in $\delta^{18}O$ data from the Greenland ice cores (Dansgaard et al., 1993). Interstadial-stadial couplets typically had a rapid onset, followed by gradual cooling (Grootes et al., 1993; Johnsen et al., 1992). Freshwater discharge to the North Atlantic increased during interstadials, likely reducing deep water formation and impacting Atlantic Meridional Overturning Circulation. Rapid transmission of a dynamic climate signal to the globe within decades was the net result (Elliot et al., 2002; Gottschalk et al., 2015), though regional response, duration and precise timing differed from the Greenland chronology.

D-O events propagated to the North Pacific (Lund and Mix, 1998), and Hendy and Kennett (2000a) have documented D-O events in the Santa Barbara Basin (SBB) with oxygen isotopes, and shifts in benthic foraminifera assemblages that support warmer SSTs during interstadials (Fig. 5a and b). Behl and Kennett (1996) noted laminations driven by anoxia during D-O interstadials. Thus, the SBB response during MIS 3 interstadials was enhanced marine temperatures, driven by increased influx of subtropical waters and weaker California Current (Hendy and Kennett, 2000a). In Owens Lake, total organic carbon apparently increased in tandem with D-O interstadials, though ascribing specific events to these %TOC fluctuations is largely speculative, due to chronological uncertainties (Benson et al., 2003, 2002).

We found a similar response in Baldwin Lake's total organic matter. Within the limits of dating uncertainties, there was apparent synchronicity between terrestrial BDL12, marine SBB, and NGRIP $\delta^{18}O$ in the timing, duration, and relative amplitude of D-O interstadials. We suggest D-O event numbers for BDL12 (Fig. 5c) after conventions of Rasmussen et al. (2014). Core gaps and noisy

organic data occurred between 60 and 52 ka, however, and winter insolation prior to 50 ka may have dampened the amplitude of potential D-O interstadials (Fig. 5c). Rasmussen et al. (2014) confirm that the North Atlantic response from 59 to 54 ka was a complex transition between global climatic states, and complex sub-intervals during D-O interstadials from this interval have been identified since initial identification and numbering. Thus, D-O interstadials 16–17 were not assigned to specific organic peaks in BDL12, but likely occurred over a 3–5 kyr interval of high-amplitude, rapid changes (Fig. 5c). Despite these caveats, millennial-scale fluctuations in Baldwin Lake organic deposition suggest that North Atlantic MIS 3 and MIS 2 perturbations were strong enough to influence Southern California climate during a period of intermediate insolation.

5.3. Pacific- and North Atlantic-induced events in California, the Great Basin, and Southwest

We examined other paleoclimate sites in California, the Great Basin, and Southwest (Fig. 6) for their response to rapid change, and asked 1) which events are coeval to environmental changes in the SBM, 2) was there a temperature and/or hydrological response at each site, and 3) is there a coherent geographic pattern of response? We focused largely on 85–20 ka, the period with the greatest number of comparative sites to BDL12, mapped in Figs. 6 and 7 with the ecoregions of Bailey (2009).

MIS 5a events in BDL12 included lowstands at 87 and 82 ka. The 82 ka event in particular was coeval with other evidence of warm conditions throughout the West, including a marine highstand along the California and Southern Oregon coasts 84–76 ka (Muhs et al., 2012). Devil's Hole experienced a maximum in $\delta^{18}O$ isotopic values (82.5 ± 0.7 ka; Moseley et al., 2016), and the onset of warm SSTs at ODP 1017 occurred 82 ka (Seki et al., 2002). Baldwin Lake rapidly transgressed after 82 ka over the course of 0.6–0.7 kyr, suggesting a sudden change in either basin deposition, or moisture regime.

Widespread climatic change next happened at terrestrial sites during the 3 kyr period spanning Heinrich Event 6 (H6, 60 ± 5 ka; Hemming, 2004) and the transition to MIS 3 (57 ka). Several terrestrial sites underwent hydrologic shifts. Lake Manley in Death Valley transitioned from mudflat to more arid saltpan ~59–57 ka (Forester et al., 2005). Runoff to Lake Babicora, located at the southernmost extent of the region shown (Fig. 6), also reduced 58 ka (Roy et al., 2013). In contrast, other sites in Southern California became wet, including Baldwin Lake's perennial lake phase throughout MIS 3, and the onset of groundwater flow in Valley Wells 60 ka (Fig. 6; Pigati et al., 2011). West of the Sierra Nevada, peak moisture included a wetter phase from 61.7 ± 0.5 to 59.8 ± 0.6 ka at McLean's Cave, with a return to relatively dry conditions afterwards (Oster et al., 2014). This demonstrated the site's a sensitivity to North Atlantic changes: Heinrich 6 (60 ± 5 ka; Hemming, 2004) coincided with wet conditions, and D-O interstadials 15–18 were arid phases in the Sierra Nevada foothills (Oster et al., 2014). Meanwhile, ice-rafted debris from increased freshwater runoff reached a maximum 59–58 ka at Mono Lake east of the Sierra Nevada (Zimmerman et al., 2011).

Thus, terrestrial hydrologic change is not uniform throughout California at the MIS 4/3 transition, though wetter sites tended to cluster in the southern sector of the Mojave Desert and the SBM. Offshore sites responded consistently with enhanced SSTs initiating close to the MIS 4/3 transition at sites1014, 1017, and 1012, but hydrologic change was difficult to determine from available records and proxy data (Hendy et al., 2004; Hendy and Kennett, 2000b; Herbert et al., 2001; Seki et al., 2002). High resolution BSi data

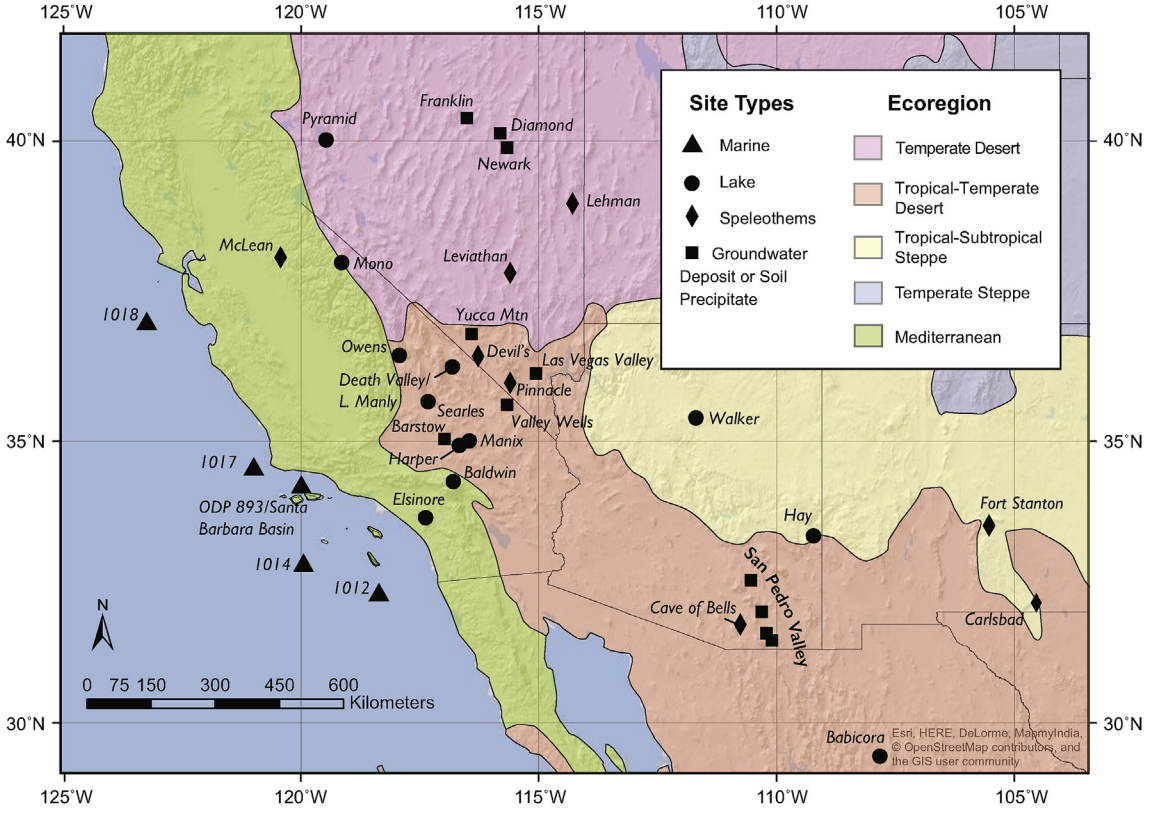

Fig. 6. Paleoclimatic sites discussed in this review, with North American ecoregions shown (Bailey, 2009). See text for references.

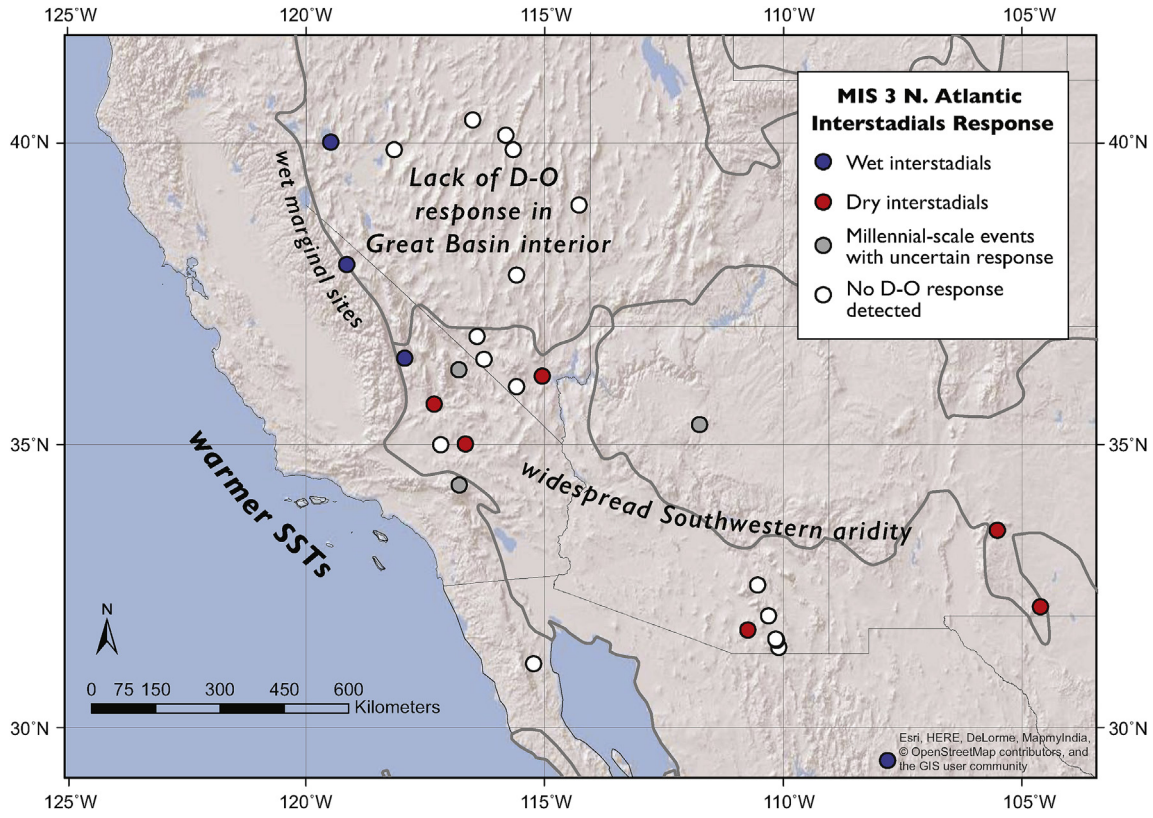

Fig. 7. Response of regional sites to Dansgaard-Oeschger (D-O) interstadials during MIS 3 (57–29 ka).

from ODP 1018 showed increasing SSTs 61 ka, and these data provide insight to other processes and moisture at the Northern California site: enhanced SSTs were accompanied with greater productivity, suppressed upwelling, and aridity that lasted 8–10 kyr (Lyle et al., 2010).

More sites span MIS 3, including recently-developed records that depend upon groundwater infiltration (e.g. speleothem records, soil precipitates, and groundwater/desert wetland deposits). We synthesize the sensitivity of paleoclimatic records to D-O interstadials, noting if the response was cold, warm, wet or dry (Fig. 7). The investigators' original climatic interpretation for D-O interstadial response were used in this map. Uncertainty in dating methods can be several millennia at sites of MIS 3 age, a recognized problem in trying to detect events that last, on average, ~1.48 kyr (Benson et al., 2003; Denniston et al., 2007; Zimmerman et al., 2011). Still, mapping current knowledge of D-O interstadial response in a large sector of the North American West did show emergent patterns, and may provide a framework for future hypothesis-testing at regional paleoclimate sites.

High-resolution marine records ODP 1017 and 1014 responded to D-O interstadials with warmer SSTs (Hendy and Kennett, 2000b; Hendy and Pedersen, 2005; Pak et al., 2012; Pospelova et al., 2015; Seki et al., 2002). Heusser (1998) detected millennial-scale increases in ODP 893 oak pollen, a dry-adapted taxa, that corresponded to D-O interstadials. Enhanced aridity was the norm during D-O interstadials at terrestrial sites, including Southwestern speleothem records Fort Stanton, Carlsbad Cavern, and Cave of the Bells (Asmerom et al., 2010; Brook et al., 2006; Wagner et al., 2010). In the tropical-temperate desert south of the Great Basin, sites demonstrate a potential sensitivity to D-O interstadials quite late, with arid fluctuations that start at 35 ka (e.g. Searles Lake, Lin et al., 1998; Las Vegas Valley, Springer et al., 2015). Sites that experienced overall greater effective moisture throughout MIS 3, but did not exhibit consistent millennial-scale variability, include Valley Wells (Pigati et al., 2011), the San Pedro Valley (Pigati et al., 2009). Records in Mexico began to show a sensitivity to D-O events by mid-MIS 3 (42–40 ka), with warmer SSTs in the Gulf of California (Price et al., 2013) and enhanced moisture at Lake Babicora (Roy et al., 2013).

The Great Basin response to D-O interstadials varied geographically, with enhanced moisture at its northern and western margins, and no apparent response towards the interior (Fig. 7). Millennial-scale oscillations were absent from Lehman, Leviathan, and Pinnacle speleothem records (Lachniet et al., 2014), and groundwater precipitates (Franklin, Newark Valley, Diamond Valley, Barstow, and Yucca Mountain, Figs. 6 and 7; Maher et al., 2014). Higher lake levels during interstadials occur at Mono, Pyramid, and Owens Lakes to the east of the Sierra Nevada (Benson et al., 2003). The northeastern Great Basin underwent saline and hypersaline oscillations in the Great Salt Lake during MIS 3 (Balch et al., 2005), and Benson et al. (2011) interpreted higher lake levels and wet D-O interstadials for this sector of the Lake Bonneville Basin. This wet response at the margins of the Great Basin may be due to nearby glaciers and the Laurentide Ice Sheet, a potential source of meltwater during warm excursions.

In the SBM, Kirby et al. (2006) previously hypothesized that D-O interstadials were wet episodes based upon laminated deposits in deep water conditions, but laminated horizons observed in BDL12 did not reliably match the organic excursions proposed as the D-O interstadials. Directly-dated relict shorelines at paleolake Manix to the north, part of the Mojave River watershed with its headwaters in the SBM, showed that D-O *stadials* were unusually wet for the region (Reheis et al., 2015). Yet with no supporting evidence in our current dataset that D-O interstadials enhanced moisture in alpine

Southern California, the hydrologic response at Baldwin Lake remains ambiguous. North of the SBM in the Mojave Desert, and eastward towards the Southwest, the geographic pattern of response to D-O interstadials was enhanced aridity (Fig. 7).

Reduced insolation, reduced evaporation, and generally wet conditions prevailed in Southern California and the Southwest at the MIS 3/2 transition at 29 ka, with some centennial-to millennial arid events. Groundwater infiltration prevailed in the Great Basin until 24 ka (Maher et al., 2014), while a highstand persisted at Owens Lake (Bacon et al., 2006) and Lake Manly (Li et al., 1996). Cave of the Bells (Wagner et al., 2010) and the San Pedro Valley sites of Pigati et al. (2009) were wet from 25 to 20 ka. An arid episode just prior to the LGM was evident at several of these sites, best documented with a well-dated, highly-resolved pollen study at Lake Elsinore that showed a ~2 kyr drought from 27.5 to 25.5 ka (Heusser et al., 2015). Other arid episodes that interrupted otherwise wet conditions include reversals at Owens Lake 25–24 ka (Bacon et al., 2006), Pyramid Lake at 29 ka (Benson et al., 2013), and a pair of lakes on the Colorado Plateau at 24.5–24 ka (Hay and Walker Lakes; Anderson et al., 2000). The high magnetic susceptibility excursion at Baldwin Lake was contemporaneous with the Lake Elsinore drought, and could have been caused by rapid sediment burial or lake mixing (Dearing, 1999).

An influx of Pacific moisture arrived in Southern California by 22 ka (Oster et al., 2015). Lake highstand and basin spillover events towards the east are events often mentioned as part of Big Bear Valley's Ice Age history (Krantz, 1983; Leidy, 2006; Stout, 1976), but the evidence has not been directly dated. Glaciation occurred for ~5 kyr on San Gorgonio, the highest-elevation peak in the SBM, depositing a series of moraines 20–16 ka and 16–15 ka (Owen et al., 2003). The early MIS 2 drought at Lake Elsinore 27.5–25.5 ka, and subsequent moisture influx ~22 ka, suggest that Southern California had a complex and dynamic hydrologic history during the Last Ice Age, with changes occurring on millennial, and perhaps submillenial, scales. Further study with tighter-resolution proxy analyses are necessary to better resolve these events in space and time.

6. Conclusions

Physical and geochemical proxy analyses on Baldwin Lake suggest that Southern California climate change was sensitive to orbitally-induced radiation over the past 125 ka, particularly in material recovered from MIS 5. Variations in local summer insolation during MIS 5e-5a (125–71 ka) were large, ranging 448–533 W/m^2, and likely the primary cause of high-amplitude shifts in lake productivity. Summer insolation was less pronounced during MIS 4–3 (71–29 ka; 465–510 W/m^2), while winter insolation was relatively stable. During the combined effects of intermediate radiation and reduced seasonal variability, portions of the North American West, particularly Southern California, experienced 1) greater effective moisture throughout MIS 3, and 2) sensitivity to North Atlantic forcing, namely Dansgaard-Oeschger (D-O) interstadial events.

The influence of D-O interstadials on California, the Great Basin, and U.S. Southwest during MIS 3–2 produced a geographically varied response. In alpine Southern California, productivity increases in the Baldwin Lake core were the apparent responses to D-O interstadials. While we have no direct measure of hydrologic change during these interstadials in the present study, enhanced aridity was a consistent response at sensitive sites in the surrounding Mojave Desert, and eastward into the Southwest. Sites on the western and northeastern margins of the Great Basin were wet during D-O interstadials, and no consistent millennial-scale events have been detected at Great Basin interior sites during MIS 3. MIS 2 brought depressed insolation and cold, glacial conditions with variable moisture. While summer insolation did not quite reach MIS 5 maxima (~530–540 W/m^2) at the MIS 2/1 transition, climate was warm and/or dry enough to cause Southern California lakes to transition to intermittent, or playa, states. Baldwin Lake has been an intermittent lake since ~12 ka.

This work highlights the sensitivity of Southern California's climate to radiative and oceanic forcing, and the need to better understand how the ocean-atmospheric system reorganizes itself to transmit such changes. It is also clear that during past climate states, radiative and oceanic forcing produced hydrologic responses that varied geographically. Improved understanding of the nature and drivers of this variability is an urgent need at present, as recent studies (e.g. Cayan et al., 2010; Diffenbaugh et al., 2015; Overpeck and Udall, 2010) forecast an increasingly warm and arid Southern California and Southwest for the rest of the 21st century. Enhanced temperature and aridity will certainly produce stresses on the region's population and ecosystems.

Acknowledgments

We are grateful for the financial support provided by the UCLA Institute of the Environment and Sustainability Presidential Fund, UCLA Graduate Division, Limnological Research Center, Geological Society of America, UCLA Dept. of Geography John Muir Memorial Endowment, Society of Woman Geographers, and the Department of the Interior Southwest Climate Science Center. Fieldwork and core recovery were greatly assisted by Katie Nelson, Scott Eliason, and Gina Griffith of the San Bernardino National Forest; Larry Winslow of Big Bear, CA; and Gregg Drilling, L.L.C. KCG especially thanks Wendy Barrera for leading IRSL subsampling and preparation at the UCLA Luminescence Laboratory, assistance from Jessica Rodysill and Kristina Brady while visiting the Limnological Research Center at the University of Minnesota, and Katherine Whitacre at Northern Arizona University's Amino Acid Geochronology Lab. We thank several students for their assistance in the field and lab, including Lauren Brown, April Chaney, Elaine Chang, Christine Hiner, Tamryn Kong, Alec Lautanen, Jennifer Leidelmeijer, Setareh Nejat, Alex Pakalniskis, Sargam Saraf, Nicole Tachiki, Marcus Thomson, Alice Wong, Alex Woodward and Renée Yun. The thorough and thoughtful comments of two anonymous reviewers greatly improved the paper, and are much appreciated. Candid conversation and feedback from many of the investigators cited, too numerous to name here, have also improved our discussion of long-term climate change in the North American West.

Appendix A. Supplementary data

Supplementary data related to this article can be found at http://dx.doi.org/10.1016/j.quascirev.2017.04.028.

References

Big Bear Lake TMDL Task Force [WWW Document], 2012. URL http://www.sawpa.org/collaboration/past-projects/big-bear-lake-tmdl-taskforce/(accessed 18 June 2014).

U.S. Climate Data, 2016. US Clim [WWW Document]. Data Big Bear Lake - Calif. URL. http://www.usclimatedata.com/climate/big-bear-lake/california/united-states/usca0094 (accessed 08 August 2016).

Ampel, L., Wohlfarth, B., Risberg, J., Veres, D., 2008. Paleolimnological response to millennial and centennial scale climate variability during MIS 3 and 2 as suggested by the diatom record in Les Echets, France. Quat. Sci. Rev. 27, 1493–1504. http://dx.doi.org/10.1016/j.quascirev.2008.04.014.

Anderson, R.S., Betancourt, J.L., Mead, J.I., Hevly, R.H., Adam, D.P., 2000. Middle- and late-Wisconsin paleobotanic and paleoclimatic records from the southern Colorado Plateau, USA. Palaeogeogr. Palaeoclimatol. Palaeoecol. 155, 31–57. http://dx.doi.org/10.1016/S0031-0182(99)00093-0.

Asmerom, Y., Polyak, V.J., Burns, S.J., 2010. Variable winter moisture in the southwestern United States linked to rapid glacial climate shifts. Nat. Geosci. 3, 114–117. http://dx.doi.org/10.1038/ngeo754.

Bacon, S.N., Burke, R.M., Pezzopane, S.K., Jayko, A.S., 2006. Last glacial maximum and Holocene lake levels of Owens Lake, eastern California, USA. Quat. Sci. Rev. 25, 1264–1282. http://dx.doi.org/10.1016/j.quascirev.2005.10.014.
Bailey, R.G., 2009. Ecosystem Geography: from Ecoregions to Sites, second ed. Springer, New York.
Balch, D.P., Cohen, A.S., Schnurrenberger, D.W., Haskell, B.J., Valero Garces, B.L., Beck, J.W., Cheng, H., Edwards, R.L., 2005. Ecosystem and paleohydrological response to Quaternary climate change in the Bonneville Basin. Utah. Palaeogeogr. Palaeoclimatol. Palaeoecol. 221, 99–122. http://dx.doi.org/10.1016/j.palaeo.2005.01.013.
Barron, J.A., Heusser, L., Herbert, T., Lyle, M., 2003. High-resolution climatic evolution of coastal northern California during the past 16,000 years. Paleoceanography 18. http://dx.doi.org/10.1029/2002PA000768 n/a-n/a.
Behl, R.J., Kennett, J.P., 1996. Brief interstadial events in the Santa Barbara basin, NE Pacific, during the past 60 kyr. Nature 379, 243–246. http://dx.doi.org/10.1038/379243a0.
Benson, L.V., Kashgarian, M., Rye, R.O., Lund, S.P., Paillet, F., Smoot, J.P., Kester, C., Mensing, S.A., Meko, D.M., Lindström, S., 2002. Holocene multidecadal and multicentennial droughts affecting northern California and Nevada. Quat. Sci. Rev. 21, 659–682.
Benson, L., Lund, S., Negrini, R., Linsley, B., Zic, M., 2003. Response of North American Great Basin lakes to dansgaard–oeschger oscillations. Quat. Sci. Rev. 22, 2239–2251. http://dx.doi.org/10.1016/S0277-3791(03)00210-5.
Benson, L.V., Lund, S.P., Smoot, J.P., Rhode, D.E., Spencer, R.J., Verosub, K.L., Louderback, L.A., Johnson, C.A., Rye, R.O., Negrini, R.M., 2011. The rise and fall of Lake Bonneville between 45 and 10.5 ka. Quat. Int 235, 57–69. http://dx.doi.org/10.1016/j.quaint.2010.12.014.
Benson, L.V., Smoot, J.P., Lund, S.P., Mensing, S.A., Foit, F.F., Rye, R.O., 2013. Insights from a synthesis of old and new climate-proxy data from the Pyramid and Winnemucca lake basins for the period 48 to 11.5 cal ka. Quat. Int. 310, 62–82. http://dx.doi.org/10.1016/j.quaint.2012.02.040.
Bird, B.W., Kirby, M.E., 2006. An alpine lacustrine record of early Holocene North American monsoon dynamics from dry lake, southern California (USA). J. Paleolimnol. 35, 179–192. http://dx.doi.org/10.1007/s10933-005-8514-3.
Blaauw, M., Christen, J.A., 2011. Flexible paleoclimate age-depth models using an autoregressive gamma process. Bayesian Anal. 6, 457–474. http://dx.doi.org/10.1214/11-BA618.
Blass, A., Bigler, C., Grosjean, M., Sturm, M., 2007. Decadal-scale autumn temperature reconstruction back to AD 1580 inferred from the varved sediments of Lake Silvaplana (southeastern Swiss Alps). Quat. Res. 68, 184–195. http://dx.doi.org/10.1016/j.yqres.2007.05.004.
Blazevic, M.A., Kirby, M.E., Woods, A.D., Browne, B.L., Bowman, D.D., 2009. A sedimentary facies model for glacial-age sediments in Baldwin Lake, Southern California. Sediment. Geol. 219, 151–168. http://dx.doi.org/10.1016/j.sedgeo.2009.05.003.
Brook, G.A., Ellwood, B.B., Railsback, L.B., Cowart, J.B., 2006. A 164 ka record of environmental change in the American Southwest from a Carlsbad Cavern speleothem. Palaeogeogr. Palaeoclimatol. Palaeoecol. 237, 483–507. http://dx.doi.org/10.1016/j.palaeo.2006.01.001.
Brunelle, A., Anderson, R.S., 2003. Sedimentary charcoal as an indicator of late-Holocene drought in the Sierra Nevada, California, and its relevance to the future. Holocene 13, 21–28. http://dx.doi.org/10.1191/0959683603hl591rp.
Burch, J.B., 1982. Freshwater Snails (Mollusca: Gastropoda) of North America (No. EPA-600/3-82-026). United States Environmental Protection Agency.
Buylaert, J.P., Murray, A.S., Thomsen, K.J., Jain, M., 2009. Testing the potential of an elevated temperature IRSL signal from K-feldspar. Radiat. Meas. 44, 560–565. http://dx.doi.org/10.1016/j.radmeas.2009.02.007.
Cacho, I., Grimalt, J.O., Pelejero, C., Canals, M., Sierro, F.J., Flores, J.A., Shackleton, N., 1999. Dansgaard-oeschger and Heinrich event imprints in alboran sea paleotemperatures. Paleoceanography 14, 698–705. http://dx.doi.org/10.1029/1999PA900044.
Cayan, D.R., Peterson, D.H., 1989. The influence of North Pacific atmospheric circulation on streamflow in the west. In: Aspects of Climate Variability in the Pacific and the Western Americas. American Geophysical Union, pp. 375–397.
Cayan, D.R., Das, T., Pierce, D.W., Barnett, T.P., Tyree, M., Gershunov, A., 2010. Future dryness in the southwest US and the hydrology of the early 21st century drought. Proc. Natl. Acad. Sci. 107, 21271–21276. http://dx.doi.org/10.1073/pnas.0912391107.
Colman, S.M., Peck, J.A., Karabanov, E.B., Carter, S.J., Bradbury, J.P., King, J.W., Williams, D.F., 1995. Continental climate response to orbital forcing from biogenic silica records in Lake Baikal. Nature 378, 769–771. http://dx.doi.org/10.1038/378769a0.
Conley, D.J., Schelske, C.L., 2002. Biogenic silica. In: Smol, J.P., Birks, H.J.B., Last, W.M., Bradley, R.S., Alverson, K. (Eds.), Tracking Environmental Change Using Lake Sediments. Kluwer Academic Publishers, Dordrecht, pp. 281–293.
Dansgaard, W., Johnsen, S.J., Clausen, H.B., Dahl-Jensen, D., Gundestrup, N.S., Hammer, C.U., Hvidberg, C.S., Steffensen, N.S., Sceinbjörnsdottir, A.E., Jouzel, J., Bond, G., 1993. Climate instability during the last interglacial period recorded in the GRIP ice core. Nature 364, 203–207. http://dx.doi.org/10.1038/364203a0.
Dean, W.E., 1974. Determination of carbonate and organic matter in calcareous sediments and sedimentary rocks by loss on ignition: comparison with other methods. SEPM J. Sediment. Res. 44 http://dx.doi.org/10.1306/74D729D2-2B21-11D7-8648000102C1865D.
Dearing, J., 1999. Environmental Magnetic Susceptibility: Using the Bartington MS2 System, second ed. Chi Publishing, Kenilworth, England.
Denniston, R.F., Asmerom, Y., Polyak, V., Dorale, J.A., Carpenter, S.J., Trodick, C., Hoye, B., González, L.A., 2007. Synchronous millennial-scale climatic changes in the Great Basin and the North Atlantic during the last interglacial. Geology 35, 619. http://dx.doi.org/10.1130/G23445A.1.
Dibblee, T.W., 1964. Geological Map of the San Gorgonio Mountain Quadrangle, San Bernardino and Riverside Counties, California. Miscellaneous Geologic Investigations.
Diffenbaugh, N.S., Swain, D.L., Touma, D., 2015. Anthropogenic warming has increased drought risk in California. Proc. Natl. Acad. Sci. 112, 3931–3936. http://dx.doi.org/10.1073/pnas.1422385112.
Elliot, M., Labeyrie, L., Duplessy, J.-C., 2002. Changes in North Atlantic deep-water formation associated with the Dansgaard–Oeschger temperature oscillations (60–10ka). Quat. Sci. Rev. 21, 1153–1165. http://dx.doi.org/10.1016/S0277-3791(01)00137-8.
Flint, L.E., Martin, P., 2012. Geohydrology of Big Bear Valley, California: Phase 1—Geologic Framework, Recharge, and Preliminary Assessment of the Source and Age of Groundwater (Scientific Investigations No. 2012–5100). U. S. Geological Survey.
Forester, R.M., Lowenstein, T.K., Spencer, R.J., 2005. An ostracode based paleolimnologic and paleohydrologic history of Death Valley: 200 to 0 ka. Geol. Soc. Am. Bull. 117, 1379. http://dx.doi.org/10.1130/B25637.1.
Garcia, A.L., Knott, J.R., Mahan, S.A., Bright, J., 2014. Geochronology and paleoenvironment of pluvial Harper lake, Mojave desert, California, USA. Quat. Res. 81, 305–317. http://dx.doi.org/10.1016/j.yqres.2013.10.008.
Georgescu, M., Moustaoui, M., Mahalov, A., Dudhia, J., 2012. Summer-time climate impacts of projected megapolitan expansion in Arizona. Nat. Clim. Change 3, 37–41. http://dx.doi.org/10.1038/nclimate1656.
Goring, S., Williams, J.E., Blois, J.L., Jackson, S.T., Paciorek, C.J., Booth, R.K., Marlon, J.R., Blaauw, M., Christen, J.A., 2012. Deposition times in the northeastern United States during the Holocene: establishing valid priors for Bayesian age models. Quat. Sci. Rev. 48, 54–60.
Gottschalk, J., Skinner, L.C., Misra, S., Waelbroeck, C., Menviel, L., Timmermann, A., 2015. Abrupt changes in the southern extent of North Atlantic deep water during dansgaard–oeschger events. Nat. Geosci. 8, 950–954. http://dx.doi.org/10.1038/ngeo2558.
Groot, M.H.M., van der Plicht, J., Hooghiemstra, H., Lourens, L.J., Rowe, H.D., 2014. Age modelling for Pleistocene lake sediments: a comparison of methods from the Andean Fúquene Basin (Colombia) case study. Quat. Geochronol. 22, 144–154. http://dx.doi.org/10.1016/j.quageo.2014.01.002.
Grootes, P.M., Stuiver, M., White, J.W.C., Johnsen, S., Jouzel, J., 1993. Comparison of oxygen isotope records from the GISP2 and GRIP Greenland ice cores. Nature 366, 552–554. http://dx.doi.org/10.1038/366552a0.
Hahn, A., Kliem, P., Ohlendorf, C., Zolitschka, B., Rosén, P., 2013. Climate induced changes as registered in inorganic and organic sediment components from Laguna Potrok Aike (Argentina) during the past 51 ka. Quat. Sci. Rev. 71, 154–166. http://dx.doi.org/10.1016/j.quascirev.2012.09.015.
Heiri, O., Lotter, A.F., Lemcke, G., 2001. Loss on ignition as a method for estimating organic and carbonate content in sediments: reproducibility and comparability of results. J. Paleolimnol. 25, 101–110.
Hemming, S.R., 2004. Heinrich events: massive late Pleistocene detritus layers of the North Atlantic and their global climate imprint. Rev. Geophys 42. http://dx.doi.org/10.1029/2003RG000128.
Hendy, I.L., Kennett, J.P., 2000a. Dansgaard-oeschger cycles and the California current system: planktonic foraminiferal response to rapid climate change in Santa Barbara Basin, ocean drilling program hole 893A. Paleoceanography 15, 30. http://dx.doi.org/10.1029/1999PA000413.
Hendy, I.L., Kennett, J.P., 2000b. Stable isotope stratigraphy and paleoceanography of the last 170 ky: site 1014, Tanner Basin, California. In: Proceedings of the Ocean Drilling Program, Scientific Results, pp. 129–140.
Hendy, I.L., Pedersen, T.F., 2005. Is pore water oxygen content decoupled from productivity on the California Margin? Trace element results from Ocean Drilling Program Hole 1017E, San Lucia slope, California: Productivity-pore water oxygen decoupling. Paleoceanography 20. http://dx.doi.org/10.1029/2004PA001123 n/a-n/a.
Hendy, I.L., Pedersen, T.F., Kennett, J.P., Tada, R., 2004. Intermittent existence of a southern Californian upwelling cell during submillennial climate change of the last 60 kyr. Paleoceanography 19. http://dx.doi.org/10.1029/2003PA000965 n/a-n/a.
Herbert, T.D., Schuffert, J., Andreasen, D., Heusser, L.E., Lyle, M., Mix, A., Ravelo, A.C., Stott, L.D., Herguera, J.C., 2001. Collapse of the California current during glacial maxima linked to climate change on land. Science 293, 71–76. http://dx.doi.org/10.1126/science.1059209.
Heusser, L., 1998. Direct correlation of millennial-scale changes in western North American vegetation and climate with changes in the California Current System over the past ~60 kyr. Paleoceanography 13, 252–262. http://dx.doi.org/10.1029/98PA00670.
Heusser, L.E., Basalm, W.L., 1977. Pollen distribution in the northeast Pacific Ocean. Quat. Res. 7, 45–62.
Heusser, L.E., Kirby, M.E., Nichols, J.E., 2015. Pollen-based evidence of extreme drought during the last Glacial (32.6–9.0 ka) in coastal southern California. Quat. Sci. Rev. 126, 242–253. http://dx.doi.org/10.1016/j.quascirev.2015.08.029.
Hodell, D.A., Schelske, C.L., Fahnenstiel, G.L., Robbins, L.L., 1998. Biologically induced calcite and its isotopic composition in Lake Ontario. Limnol. Oceanogr. 43, 187–199.
Hooghiemstra, H., Lézine, A.-M., Leroy, S.A.G., Dupont, L., Marret, F., 2006. Late

Quaternary palynology in marine sediments: a synthesis of the understanding of pollen distribution patterns in the NW African setting. Quat. Int. 148, 29–44. http://dx.doi.org/10.1016/j.quaint.2005.11.005.
Hu, F.S., Kaufman, D.S., Yoneji, S., Nelson, D., Shemesh, A., Huang, Y., Tian, J., Bond, G., Clegg, B., Brown, T., 2003. Cyclic variation and solar forcing of Holocene climate in the alaskan subarctic. Science 301, 1890–1893. http://dx.doi.org/10.1126/science.1088568.
Imbrie, J., Hays, J.D., Martinson, D.G., McIntyre, A., Mix, A.C., Morley, J.J., Pisias, N., Prell, W.L., Shackleton, N.J., 1984. The orbital theory of Pleistocene climate: support from a revised chronology of the marine delta18O record. In: Ilankovitch and Climate: Understanding the Response to Astronomical Forcing, p. 269.
Jiménez-Moreno, G., Anderson, R.S., Desprat, S., Grigg, L.D., Grimm, E.C., Heusser, L.E., Jacobs, B.F., López-Martínez, C., Whitlock, C.L., Willard, D.A., 2010. Millennial-scale variability during the last glacial in vegetation records from North America. Quat. Sci. Rev. 29, 2865–2881. http://dx.doi.org/10.1016/j.quascirev.2009.12.013.
Johnsen, S.J., Clausen, H.B., Dansgaard, W., Fuhrer, K., Gundestrup, N., Hammer, C.U., Iversen, P., Jouzel, J., Stauffer, B., steffensen, J.P., 1992. Irregular glacial interstadials recorded in a new Greenland ice core. Nature 359, 311–313. http://dx.doi.org/10.1038/359311a0.
Kaplan, M.R., Wolfe, A.P., Miller, G.H., 2002. Holocene environmental variability in southern Greenland inferred from lake sediments. Quat. Res. 58, 149–159. http://dx.doi.org/10.1006/qres.2002.2352.
Kirby, M.E., Lund, S.P., Bird, B.W., 2006. Mid-Wisconsin sediment record from Baldwin Lake reveals hemispheric climate dynamics (Southern CA, USA). Palaeogeogr. Palaeoclimatol. Palaeoecol. 241, 267–283. http://dx.doi.org/10.1016/j.palaeo.2006.03.043.
Kirby, M.E., Lund, S.P., Anderson, M.A., Bird, B.W., 2007. Insolation forcing of Holocene climate change in Southern California: a sediment study from Lake Elsinore. J. Paleolimnol. 38, 395–417. http://dx.doi.org/10.1007/s10933-006-9085-7.
Kirby, M.E., Zimmerman, S.R.H., Patterson, W.P., Rivera, J.J., 2012. A 9170-year record of decadal-to-multi-centennial scale pluvial episodes from the coastal Southwest United States: a role for atmospheric rivers? Quat. Sci. Rev. 46, 57–65. http://dx.doi.org/10.1016/j.quascirev.2012.05.008.
Kirby, M.E., Feakins, S.J., Bonuso, N., Fantozzi, J.M., Hiner, C.A., 2013. Latest Pleistocene to Holocene hydroclimates from Lake Elsinore, California. Quat. Sci. Rev. 76, 1–15. http://dx.doi.org/10.1016/j.quascirev.2013.05.023.
Kirby, M.E., Knell, E.J., Anderson, W.T., Lachniet, M.S., Palermo, J., Eeg, H., Lucero, R., Murrieta, R., Arevalo, A., Silveira, E., Hiner, C.A., 2015. Evidence for insolation and pacific forcing of late glacial through Holocene climate in the central Mojave desert (silver lake, CA). Quat. Res. 84, 174–186. http://dx.doi.org/10.1016/j.yqres.2015.07.003.
Krantz, T., 1983. The pebble plains of Baldwin Lake. Fremontia 10, 9–13.
Kylander, M.E., Ampel, L., Wohlfarth, B., Veres, D., 2011. High-resolution X-ray fluorescence core scanning analysis of Les Echets (France) sedimentary sequence: new insights from chemical proxies. J. Quat. Sci. 26, 109–117. http://dx.doi.org/10.1002/jqs.1438.
Lachniet, M.S., Denniston, R.F., Asmerom, Y., Polyak, V.J., 2014. Orbital control of western North America atmospheric circulation and climate over two glacial cycles. Nat. Commun. 5 http://dx.doi.org/10.1038/ncomms4805.
Laskar, J., Robutel, P., Joutel, F., Gastineau, M., Correia, A.C.M., Levrard, B., 2004. A long-term numerical solution for the insolation quantities of the Earth. Astron. Astrophys 428, 261–285. http://dx.doi.org/10.1051/0004-6361:20041335.
Lawson, M.J., Roder, B.J., Stang, D.M., Rhodes, E.J., 2012. OSL and IRSL characteristics of quartz and feldspar from southern California, USA. Radiat. Meas. 47, 830–836. http://dx.doi.org/10.1016/j.radmeas.2012.03.025.
Leidy, R., 2006. Prehistoric and Historic Environmental Conditions in Bear Valley, San Bernardino County, California (Sacramento, CA).
Li, J., Lowenstein, T.K., Brown, C.B., Ku, T.-L., Luo, S., 1996. A 100 ka record of water tables and paleoclimates from salt cores, Death Valley, California. Palaeogeogr. Palaeoclimatol. Palaeoecol. 123, 179–203. http://dx.doi.org/10.1016/0031-0182(95)00123-9.
Lin, J.C., Broecker, W.S., Hemming, S.R., Hajdas, I., Anderson, R.F., Smith, G.I., Kelley, M., Bonani, G., 1998. A reassessment of U-Th and14C ages for late-glacial high-frequency hydrological events at Searles Lake, California. Quat. Res. 49, 11–23. http://dx.doi.org/10.1006/qres.1997.1949.
Lund, D.C., Mix, A.C., 1998. Millennial-scale deep water oscillations: reflections of the North Atlantic in the deep Pacific from 10 to 60 ka. Paleoceanography 13, 10–19. http://dx.doi.org/10.1029/97PA02984.
Lyle, M., Heusser, L., Ravelo, C., Andreasen, D., Olivarez Lyle, A., Diffenbaugh, N., 2010. Pleistocene water cycle and eastern boundary current processes along the California continental margin. Paleoceanography 25. http://dx.doi.org/10.1029/2009PA001836.
MacDonald, G.M., Case, R.A., 2005. Variations in the pacific decadal oscillation over the past millennium. Geophys. Res. Lett. 32 http://dx.doi.org/10.1029/2005GL022478.
MacDonald, G.M., Moser, K.A., Bloom, A.M., Porinchu, D.F., Potito, A.P., Wolfe, B.B., Edwards, T.W.D., Petel, A., Orme, A.R., Orme, A.J., 2008. Evidence of temperature depression and hydrological variations in the eastern Sierra Nevada during the Younger Dryas stade. Quat. Res. 70, 131–140. http://dx.doi.org/10.1016/j.yqres.2008.04.005.
Mahan, S.A., Gray, H.J., Pigati, J.S., Wilson, J., Lifton, N.A., Paces, J.B., Blaauw, M., 2014. A geochronologic framework for the Ziegler Reservoir fossil site, Snowmass Village, Colorado. Quat. Res. 82, 490–503. http://dx.doi.org/10.1016/j.yqres.2014.03.004.
Maher, K., Ibarra, D.E., Oster, J.L., Miller, D.M., Redwine, J.L., Reheis, M.C., Harden, J.W., 2014. Uranium isotopes in soils as a proxy for past infiltration and precipitation across the western. United States. Am. J. Sci. 314, 821–857. http://dx.doi.org/10.2475/04.2014.01.
McKay, N.P., Kaufman, D.S., Michelutti, N., 2008. Biogenic silica concentration as a high-resolution, quantitative temperature proxy at Hallet Lake, south-central Alaska. Geophys. Res. Lett. 35 http://dx.doi.org/10.1029/2007GL032876.
Melles, M., Brigham-Grette, J., Glushkova, O.Y., Minyuk, P.S., Nowaczyk, N.R., Hubberten, H.-W., 2006. Sedimentary geochemistry of core PG1351 from Lake El'gygytgyn—a sensitive record of climate variability in the East Siberian Arctic during the past three glacial–interglacial cycles. J. Paleolimnol. 37, 89–104. http://dx.doi.org/10.1007/s10933-006-9025-6.
Mensing, S.A., Sharpe, S.E., Tunno, I., Sada, D.W., Thomas, J.M., Starratt, S., Smith, J., 2013. The Late Holocene Dry Period: multiproxy evidence for an extended drought between 2800 and 1850 cal yr BP across the central Great Basin, USA. Quat. Sci. Rev. 78, 266–282. http://dx.doi.org/10.1016/j.quascirev.2013.08.010.
Minnich, R.A., 1984. Snow drifting and timberline dynamics on mount san Gorgonio, California, U.S.A. Arct. Alp. Res. 16, 395. http://dx.doi.org/10.2307/1550901.
Morton, D.M., Miller, F.K., 2006. Geologic Map of the San Bernardino and Santa Ana 30' x 60' Quadrangles, California (Open-file No. 2006–1217). U. S. Geological Survey.
Moseley, G.E., Edwards, R.L., Wendt, K.A., Cheng, H., Dublyansky, Y., Lu, Y., Boch, R., Spotl, C., 2016. Reconciliation of the Devils Hole climate record with orbital forcing. Science 351, 165–168. http://dx.doi.org/10.1126/science.aad4132.
Muhs, D.R., Simmons, K.R., Schumann, R.R., Groves, L.T., Mitrovica, J.X., Laurel, D., 2012. Sea-level history during the Last Interglacial complex on San Nicolas Island, California: implications for glacial isostatic adjustment processes, paleozoogeography and tectonics. Quat. Sci. Rev. 37, 1–25. http://dx.doi.org/10.1016/j.quascirev.2012.01.010.
National Oceanic and Atmospheric Administration, n.d. Climate – Southern California Average Annual Precipitation. [WWW Document]. URL http://www.wrh.noaa.gov/sgx/climate/pcpn-avg.php?wfo=sgx.
Nowaczyk, N.R., Melles, M., Minyuk, P., 2006. A revised age model for core PG1351 from Lake El'gygytgyn, Chukotka, based on magnetic susceptibility variations tuned to northern hemisphere insolation variations. J. Paleolimnol. 37, 65–76. http://dx.doi.org/10.1007/s10933-006-9023-8.
Nussbaumer, S.U., Steinhilber, F., Trachsel, M., Breitenmoser, P., Beer, J., Blass, A., Grosjean, M., Hafner, A., Holzhauser, H., Wanner, H., Zumbühl, H.J., 2011. Alpine climate during the Holocene: a comparison between records of glaciers, lake sediments and solar activity. J. Quat. Sci. 26, 703–713. http://dx.doi.org/10.1002/jqs.1495.
Oster, J.L., Kelley, N.P., 2016. Tracking regional and global teleconnections recorded by western North American speleothem records. Quat. Sci. Rev. 149, 18–33. http://dx.doi.org/10.1016/j.quascirev.2016.07.009.
Oster, J.L., Montañez, I.P., Mertz-Kraus, R., Sharp, W.D., Stock, G.M., Spero, H.J., Tinsley, J., Zachos, J.C., 2014. Millennial-scale variations in western Sierra Nevada precipitation during the last glacial cycle MIS 4/3 transition. Quat. Res. 82, 236–248. http://dx.doi.org/10.1016/j.yqres.2014.04.010.
Oster, J.L., Ibarra, D.E., Winnick, M.J., Maher, K., 2015. Steering of westerly storms over western north America at the last glacial maximum. Nat. Geosci. 8, 201–205. http://dx.doi.org/10.1038/ngeo2365.
Overpeck, J., Udall, B., 2010. Dry times ahead. Science 328, 1642–1643. http://dx.doi.org/10.1126/science.1186591.
Overpeck, J., Garfin, G., Jardine, A., Busch, D.E., Cayan, D., Dettinger, M., Fleishman, E., Gershunov, A., MacDonald, G., Redmond, K.T., Travis, W.R., Udall, B., 2013. Summary for decision makers. In: Garfin, G., Jardine, A., Merideth, R., Black, M., LeRoy, S. (Eds.), Assessment of Climate Change in the Southwest United States. Island Press/Center for Resource Economics, Washington, DC, pp. 1–20.
Owen, L.A., Finkel, R.C., Minnich, R.A., Perez, A.E., 2003. Extreme southwestern margin of late Quaternary glaciation in North America: timing and controls. Geology 31, 729. http://dx.doi.org/10.1130/G19561.1.
Pak, D.K., Lea, D.W., Kennett, J.P., 2012. Millennial scale changes in sea surface temperature and ocean circulation in the northeast Pacific, 10–60 kyr BP: CA margin millennial scale events. Paleoceanography 27. http://dx.doi.org/10.1029/2011PA002238 n/a-n/a.
Paladino, L., 2008. A Vegetation Reconstruction of Big Bear Lake: Local Changes and Inferred Regional Climatology. UCLA, Los Angeles.
Phillips, F.M., Zreda, M.G., Benson, L.V., Plummer, M.A., Elmore, D., Sharma, P., 1996. Chronology for fluctuations in late Pleistocene Sierra Nevada glaciers and lakes. Science 274, 749–751. http://dx.doi.org/10.1126/science.274.5288.749.
Pigati, J.S., Bright, J.E., Shanahan, T.M., Mahan, S.A., 2009. Late Pleistocene paleohydrology near the boundary of the sonoran and chihuahuan deserts, southeastern Arizona, USA. Quat. Sci. Rev. 28, 286–300. http://dx.doi.org/10.1016/j.quascirev.2008.09.022.
Pigati, J.S., Miller, D.M., Bright, J.E., Mahan, S.A., Nekola, J.C., Paces, J.B., 2011. Chronology, sedimentology, and microfauna of groundwater discharge deposits in the central Mojave Desert, Valley Wells, California. Geol. Soc. Am. Bull. 123, 2224–2239. http://dx.doi.org/10.1130/B30357.1.
Pospelova, V., Price, A.M., Pedersen, T.F., 2015. Palynological evidence for late Quaternary climate and marine primary productivity changes along the California margin: climate and primary productivity on CM. Paleoceanography 30, 877–894. http://dx.doi.org/10.1002/2014PA002728.
Price, A.M., Mertens, K.N., Pospelova, V., Pedersen, T.F., Ganeshram, R.S., 2013. Late

Quaternary Climatic and Oceanographic Changes in the Northeast Pacific as Recorded by Dinoflagellate Cysts from Guaymas Basin, Gulf of California (Mexico): dinoflagellate cysts from Guaymas Basin. Paleoceanography 28, 200–212. http://dx.doi.org/10.1002/palo.20019.

Prokopenko, A.A., Hinnov, L.A., Williams, D.F., Kuzmin, M.I., 2006. Orbital forcing of continental climate during the Pleistocene: a complete astronomically tuned climatic record from Lake Baikal, SE Siberia. Quat. Sci. Rev. 25, 3431–3457. http://dx.doi.org/10.1016/j.quascirev.2006.10.002.

Rack, F.R., Heise, E.A., Stein, R., 1995. Magnetic susceptibility and physical properties of sediment cores from site 893, Santa Barbara Basin: records of sediment diagenesis or of paleoclimatic and paleoceanographic change?. In: In Proceedings of the Ocean Drilling Program, Scientific Results.

Rasmussen, S.O., Bigler, M., Blockley, S.P., Blunier, T., Buchardt, S.L., Clausen, H.B., Cvijanovic, I., Dahl-Jensen, D., Johnsen, S.J., Fischer, H., Gkinis, V., Guillevic, M., Hoek, W.Z., Lowe, J.J., Pedro, J.B., Popp, T., Seierstad, I.K., Steffensen, J.P., Svensson, A.M., Vallelonga, P., Vinther, B.M., Walker, M.J.C., Wheatley, J.J., Winstrup, M., 2014. A stratigraphic framework for abrupt climatic changes during the Last Glacial period based on three synchronized Greenland ice-core records: refining and extending the INTIMATE event stratigraphy. Quat. Sci. Rev. 106, 14–28. http://dx.doi.org/10.1016/j.quascirev.2014.09.007.

Reheis, M.C., Miller, D.M., McGeehin, J.P., Redwine, J.R., Oviatt, C.G., Bright, J., 2015. Directly dated MIS 3 lake-level record from lake Manix, Mojave desert, California, USA. Quat. Res. 83, 187–203. http://dx.doi.org/10.1016/j.yqres.2014.11.003.

Reimer, P., 2013. IntCal13 and Marine13 radiocarbon age calibration curves 0–50,000 Years cal BP. Radiocarbon 55, 1869–1887. http://dx.doi.org/10.2458/azu_js_rc.55.16947.

Retelle, M., Child, J., 1996. Suspended sediment transport and deposition in a high arctic meromictic lake. J. Paleolimnol. 16 http://dx.doi.org/10.1007/BF00176933.

Rhodes, E.J., 2015. Dating sediments using potassium feldspar single-grain IRSL: initial methodological considerations. Quat. Int. 362, 14–22. http://dx.doi.org/10.1016/j.quaint.2014.12.012.

Rood, D.H., Burbank, D.W., Finkel, R.C., 2011. Chronology of glaciations in the Sierra Nevada, California, from 10Be surface exposure dating. Quat. Sci. Rev. 30, 646–661. http://dx.doi.org/10.1016/j.quascirev.2010.12.001.

Roy, P.D., Quiroz-Jiménez, J.D., Pérez-Cruz, L.L., Lozano-García, S., Metcalfe, S.E., Lozano-Santacruz, R., López-Balbiaux, N., Sánchez-Zavala, J.L., Romero, F.M., 2013. Late Quaternary paleohydrological conditions in the drylands of northern Mexico: a summer precipitation proxy record of the last 80 cal ka BP. Quat. Sci. Rev. 78, 342–354. http://dx.doi.org/10.1016/j.quascirev.2012.11.020.

Schnurrenberger, D., Russell, J., Kelts, K., 2003. Classification of lacustrine sediments based on sedimentary components. J. Paleolimnol. 29, 141–154. http://dx.doi.org/10.1023/A:1023270324800.

Seki, O., Ishiwatari, R., Matsumoto, K., 2002. Millennial climate oscillations in NE Pacific surface waters over the last 82 kyr: new evidence from alkenones: alkenone sea surface temperature in California margin. Geophys. Res. Lett. 29 http://dx.doi.org/10.1029/2002GL015200, 59–1-59–4.

Silveira, E.I., 2014. Reconstructing Hydrologic Change over the Past 96,000 Years Using Sediments from Baldwin Lake, San Bernardino County, California (B.A. Thesis). CSU-Fullerton, Fullerton, CA.

Springer, K.B., Manker, C.R., Pigati, J.S., 2015. Dynamic response of desert wetlands to abrupt climate change. Proc. Natl. Acad. Sci. 112, 14522–14526. http://dx.doi.org/10.1073/pnas.1513352112.

Stout, M.L., 1976. Geologic Guide to the San Bernardino Mountains, Southern California: Annual Spring Field Trip.

Street, J.H., Anderson, R.S., Paytan, A., 2012. An organic geochemical record of Sierra Nevada climate since the LGM from Swamp Lake, Yosemite. Quat. Sci. Rev. 40, 89–106. http://dx.doi.org/10.1016/j.quascirev.2012.02.017.

Tubbs, A.M., 1972. Summer thunderstorms over southern California. Mon. Weather Rev. 100, 799–807. doi:10.1175/1520-0493(1972)100<0799:STOSC>2.3.CO;2

Tzedakis, P.C., Andrieu, V., de Beaulieu, J.-L., Birks, H.J.B., Crowhurst, S., Follieri, M., Hooghiemstra, H., Magri, D., Reille, M., Sadori, L., Shackleton, N.J., Wijmstra, T.A., 2001. Establishing a terrestrial chronological framework as a basis for biostratigraphical comparisons. Quat. Sci. Rev. 20, 1583–1592. http://dx.doi.org/10.1016/S0277-3791(01)00025-7.

Vogel, H., Meyer-Jacob, C., Melles, M., Brigham-Grette, J., Andreev, A.A., Wennrich, V., Tarasov, P.E., Rosén, P., 2013. Detailed insight into Arctic climatic variability during MIS 11c at Lake El'gygytgyn, NE Russia. Clim. Past. 9, 1467–1479. http://dx.doi.org/10.5194/cp-9-1467-2013.

Wagner, J.D.M., Cole, J.E., Beck, J.W., Patchett, P.J., Henderson, G.M., Barnett, H.R., 2010. Moisture variability in the southwestern United States linked to abrupt glacial climate change. Nat. Geosci. 3, 110–113. http://dx.doi.org/10.1038/ngeo707.

Wise, E.K., 2010. Spatiotemporal variability of the precipitation dipole transition zone in the western United States: PRECIPITATION DIPOLE TRANSITION ZONE. Geophys. Res. Lett. 37 http://dx.doi.org/10.1029/2009GL042193 n/a-n/a.

Wohlfarth, B., Veres, D., Ampel, L., Lacourse, T., Blaauw, M., Preusser, F., Andrieu-Ponel, V., Kéravis, D., Lallier-Vergès, E., Björck, S., Davies, S.M., de Beaulieu, J.-L., Risberg, J., Hormes, A., Kasper, H.U., Possnert, G., Reille, M., Thouveny, N., Zander, A., 2008. Rapid ecosystem response to abrupt climate changes during the last glacial period in western Europe, 40–16 ka. Geology 36, 407. http://dx.doi.org/10.1130/G24600A.1.

Woodhouse, C.A., Meko, D.M., MacDonald, G.M., Stahle, D.W., Cook, E.R., 2010. A 1,200-year perspective of 21st century drought in southwestern North America. Proc. Natl. Acad. Sci. 107, 21283–21288. http://dx.doi.org/10.1073/pnas.0911197107.

Woolfenden, W.B., 2003. A 180,000-year pollen record from Owens Lake, CA: terrestrial vegetation change on orbital scales. Quat. Res. 59, 430–444. http://dx.doi.org/10.1016/S0033-5894(03)00033-4.

Zimmerman, S.H., Myrbo, A., 2015. Lacustrine Environments (14 C)., in: Encyclopedia of Scientific Dating Methods, pp. 365–371.

Zimmerman, S.R.H., Pearl, C., Hemming, S.R., Tamulonis, K., Hemming, N.G., Searle, S.Y., 2011. Freshwater control of ice-rafted debris in the last glacial period at Mono Lake, California, USA. Quat. Res. 76, 264–271. http://dx.doi.org/10.1016/j.yqres.2011.06.003.